Design and synthesis of novel SCM-198 analogs as cardioprotective agents: Structure-activity relationship studies and biological evaluations

Shanshan Luo, Shengtao Xu, Junkai Liu, Fenfen Ma, Yi Zhun Zhu

PII: S0223-5234(20)30440-2

DOI: https://doi.org/10.1016/j.ejmech.2020.112469

Reference: EJMECH 112469

To appear in: *European Journal of Medicinal Chemistry*

Received Date: 7 April 2020

Revised Date: 11 May 2020

Accepted Date: 13 May 2020

Please cite this article as: S. Luo, S. Xu, J. Liu, F. Ma, Y.Z. Zhu, Design and synthesis of novel SCM-198 analogs as cardioprotective agents: Structure-activity relationship studies and biological evaluations, *European Journal of Medicinal Chemistry* (2020), doi: https://doi.org/10.1016/j.ejmech.2020.112469.

Graphic Abstract

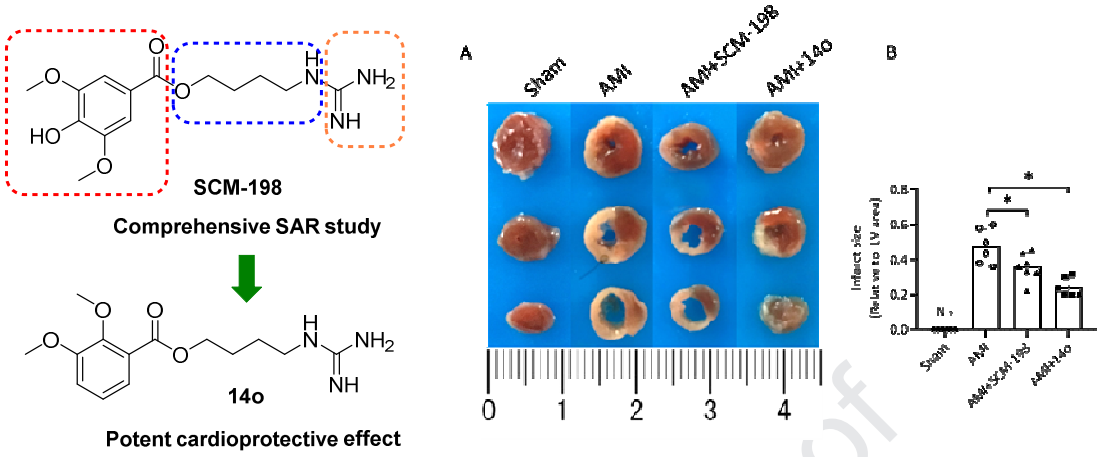

Design and Synthesis of Novel SCM-198 Analogs as Cardioprotective Agents: Structure-Activity Relationship Studies and Biological Evaluations

Shanshan Luo,[a,d,e,1] Shengtao Xu,[b,1] Junkai Liu,[b] Fenfen Ma,[c] and Yi Zhun Zhu[d,e,*]

[a] Key Laboratory of Cardiovascular and Cerebrovascular Medicine, Nanjing Medical University, 101 Longmian Avenue, Nanjing 211166, P. R. China

[b] State Key Laboratory of Natural Medicines and Department of Medicinal Chemistry, China Pharmaceutical University, 24 Tong Jia Xiang, Nanjing 210009, P. R. China

[c] Department of Pharmacy, Shanghai Pudong Hospital, Fudan University, Shanghai 201399, P. R. China

[d] Pharmacy and State Key Laboratory of Quality Research in Chinese Medicine, Macau University of Science and Technology, Macau, P. R. China

[e] Department of Pharmacology, School of pharmacy, Fudan University, Shanghai 200032, P. R. China

Abstract:

SCM-198 (Leonurine) has attracted great attention due to its cardioprotective effects in myocardial infarction (MI). However, no systematic modifications and structure-activity relationship (SAR) studies could be traced so far. In this study, 35 analogs of SCM-198 were designed, synthesized and their cardioprotective effects were evaluated. The cell viability assay on cardiomyocyte cell line H9c2 challenged with H_2O_2 showed that several analogs exhibited more potent cytoprotective effects than SCM-198 at 1 μM and 10 μM concentrations. LDH release level in cells treated with 1 μM **14o** was comparable with cells treated with 10 μM SCM-198. Results of Bcl-2 expression and caspase-3 activation accordingly indicated higher protective activity of **14o** than SCM-198. Moreover, in a mouse model of MI, the mice pretreated with **14o** had much lower infarct size compared with that of SCM-198. The mechanism study suggested that **14o** improved cardiac morphology and reduced apoptosis of cardiomyocytes in the border zone of infarction, as proved by H&E and

TUNEL staining.

Keywords: SCM-198; leonurine; cardioprotection; myocardial infarction; structural modification

1. Introduction

Although considerable improvements have occurred in the treatment of cardiovascular disease (CVD), it still produces immense health and economic burden globally and will become even more prevalent as the population ages. CVD is now the first cause of death globally, taking an estimated 17.9 million lives annually calculated from the World Health Organization (WHO) [1]. Acute myocardial infarction (AMI) is one of the most deadly causes of CVD-induced death and is becoming an increasingly significant problem in developing countries [2]. AMI mainly caused by coronary artery stenosis or thrombosis, and ischemia in the nearly blood supplying areas results in corresponding hypoxic injury of cardiomyocytes. Apart from surgical treatment, development of effective drugs that can reduce infarct area and improve prognosis is likely to contribute to the reduction in the fatality from CVD, possibly leading to new treatment options [3].

Natural products have long been an important source of novel drugs or leads [4]. Many natural products and their derivatives have been successfully developed for clinical application to treat human diseases in almost all therapeutic areas [5]. SCM-198 (synonyms: leonurine, Figure 1) is a natural alkaloid isolated from *Herba leonuri*, which has been widely used in Chinese traditional medicine for hundreds of years to treat dysmenorrhea, menoxenia and some other gynecological disorders [6]. During the last two decades, we have shown that SCM-198 can regulate a variety of pathological processes including oxidative stress, fibrosis, inflammation, apoptosis, and multiple cardiovascular diseases [7]. In particular, we have identified the cardiovascular and cerebrovascular protective effects of SCM-198 and its derivatives in rat model of MI and stroke [8-10]. Mechanism studies revealed that SCM-198 exhibited cardioprotective effects against ischemic injury in various ways mainly via

anti-oxidative and anti-apoptotic activities in these models and could preserve the activity of Mn-containing superoxide dismutase (MnSOD) [11-12]. The promising cardioprotective effects, low toxicity and appropriate pharmacokinetic characteristics of SCM-198, make it a potential drug candidate to treat CVD [13]. Our recent promising pharmacological results of SCM-198 guaranteed the approval of its clinical trials in China as a cardioprotective agent for patients with atherosclerosis [14].

Despite the promising properties of SCM-198 as a good lead compound for the development of novel cardioprotective agents, its SARs are still poorly understood, which largely hampered its further clinical applications and the discovery of more favorable cardioprotective agents. Previously, some conjugates of SCM-198, including SCM-198/cysteine (**1**, Figure 1) [15], SCM-198/aspirin (**2**) [16], SCM-198/glucuronide (**3**) [17] and some dimers [18-19] were reported by our group, which exhibited more potent anti-myocardial ischemia activities. Inspired by these encouraging results and the absence of a comprehensive structural modification of SCM-198, we speculated that the systematic structural modification of SCM-198 and further SAR analysis may be a potential way to develop novel cardioprotective agents with improved pharmacological efficacy and druggability. [20]

Herein, we wish to report the results of SAR trends of SCM-198 for cardioprotection against AMI. In the present study, a series of analogs of SCM-198 were designed and synthesized, some compounds showed excellent cardioprotective activities. Particularly, compound **14o** exhibited much more potent *in vivo* potency in AMI models than SCM-198 as well as applicable pharmacokinetic profiles, which deserved further development as a cardioprotective agent.

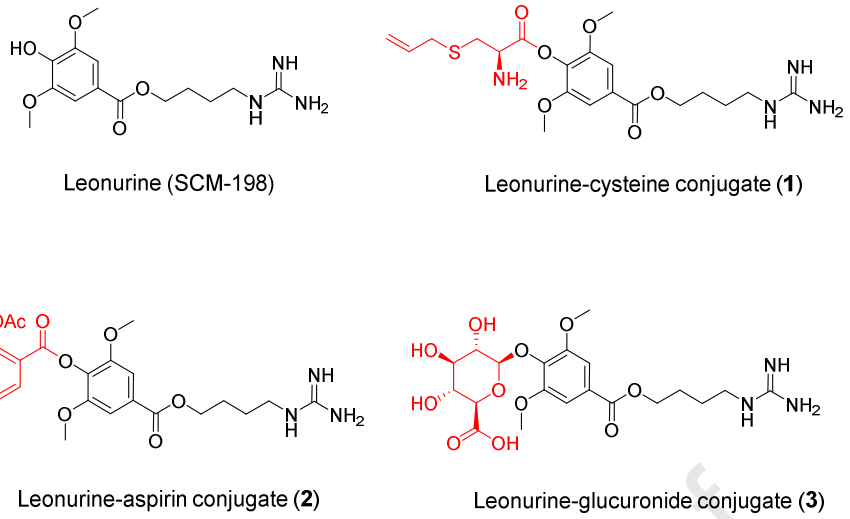

Figure 1. Structures of SCM-198 and its conjugates synthesized in our lab.

2. Results and discussion

2.1 Chemistry

The novel SCM-198 analogs were designed by replacing the linker, aromatic ring, and guanidine group of SCM-198. As shown in Scheme 1, analogs **11a-h** were characterized by the replacement of the butanolamine linker of SCM-198 with various amino alcohols. Methyl-isothiourea (**4**) was protected with Boc protection group first to afford *N,N'*-Boc-metyl-isothiourea (**5**), which was followed by reaction with various amino alcohols, yielding compounds **6a-h** in almost quantitive yields without column chromatography. Condensation of the alcohols **6a-h** with acetylated syringate (**8**) led to aryl esters **9a-h** in excellent yields. Hydrolysis of the acetyl group and subsequent removal of Boc groups by zinc bromide in dichloromethane (DCM) gave target compounds **11a-h** in good yields. It should be noted that the traditional deprotection method using trifluoroacetic acid (TFA) or HCl caused a certain degree of decompose of the target compounds.

Scheme 1. Synthesis of SCM-198 analogs **11a-h**[a]

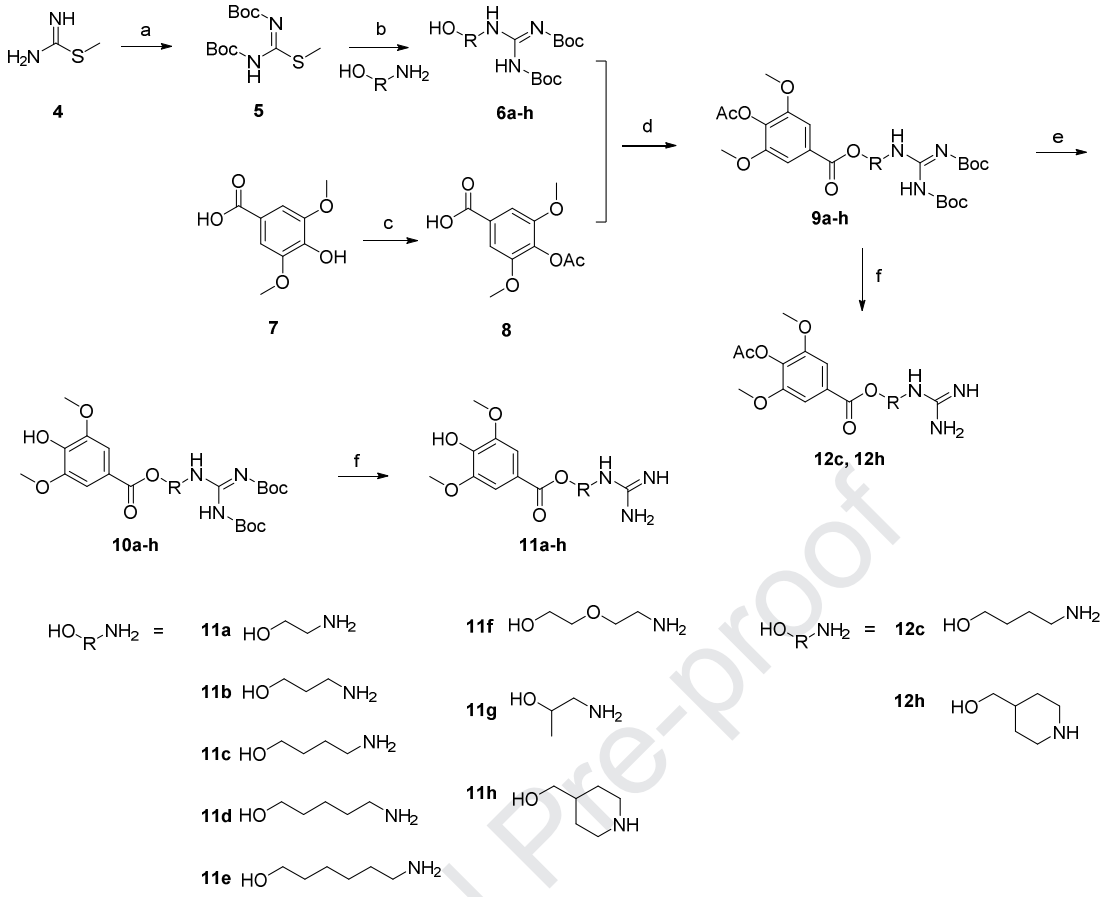

[a]Reagents and conditions: (a) $(Boc)_2O$, $NaHCO_3$, DCM, r.t., 7 d, 96%; (b) corresponding amino alcohols, DMF, r.t., 12-24 h, 95-99%; (c) Ac_2O, TEA, DCM, r.t., 5 h, 97%; (d) EDCI, DMAP, DCM, r.t., 0.5-12 h, 92-96%; (e) NaOH, MeOH, r.t., 5-10 min, 82-90%; (f) $ZnBr_2$, DCM, r.t., 1-12 h, 71-95%.

The second series of analogs were prepared by the replacement of 4-hydroxy 3,5-dimethoxybenzoic acid in SCM-198 with a panel of different acids including aliphatic acids (**14a-b**), heterocyclic acids (**14c-e**) and aromatic acids (**14f-t**). As shown in Scheme 2, those target compounds can be obtained from the condensation of different acids in a similar method as described above. Finally, in the third series of compounds, structural modifications were focused on the alternatives to the guanidine group of SCM-198 (Scheme 3). Compounds **17a-d** were prepared from simple coupling reaction between acetylated syringate (**8**) and various amino alcohols, followed by hydrolysis of the acetyl group. Besides, de-guanidine product 4-hydroxy-3,5-dimethoxy-benzoic acid 4-amino-butyl ester (**19**) was synthesized by

the deprotection of **18**, which was obtained *via* the method described above.

Scheme 2. Synthesis of SCM-198 analogs **14a-t**[a]

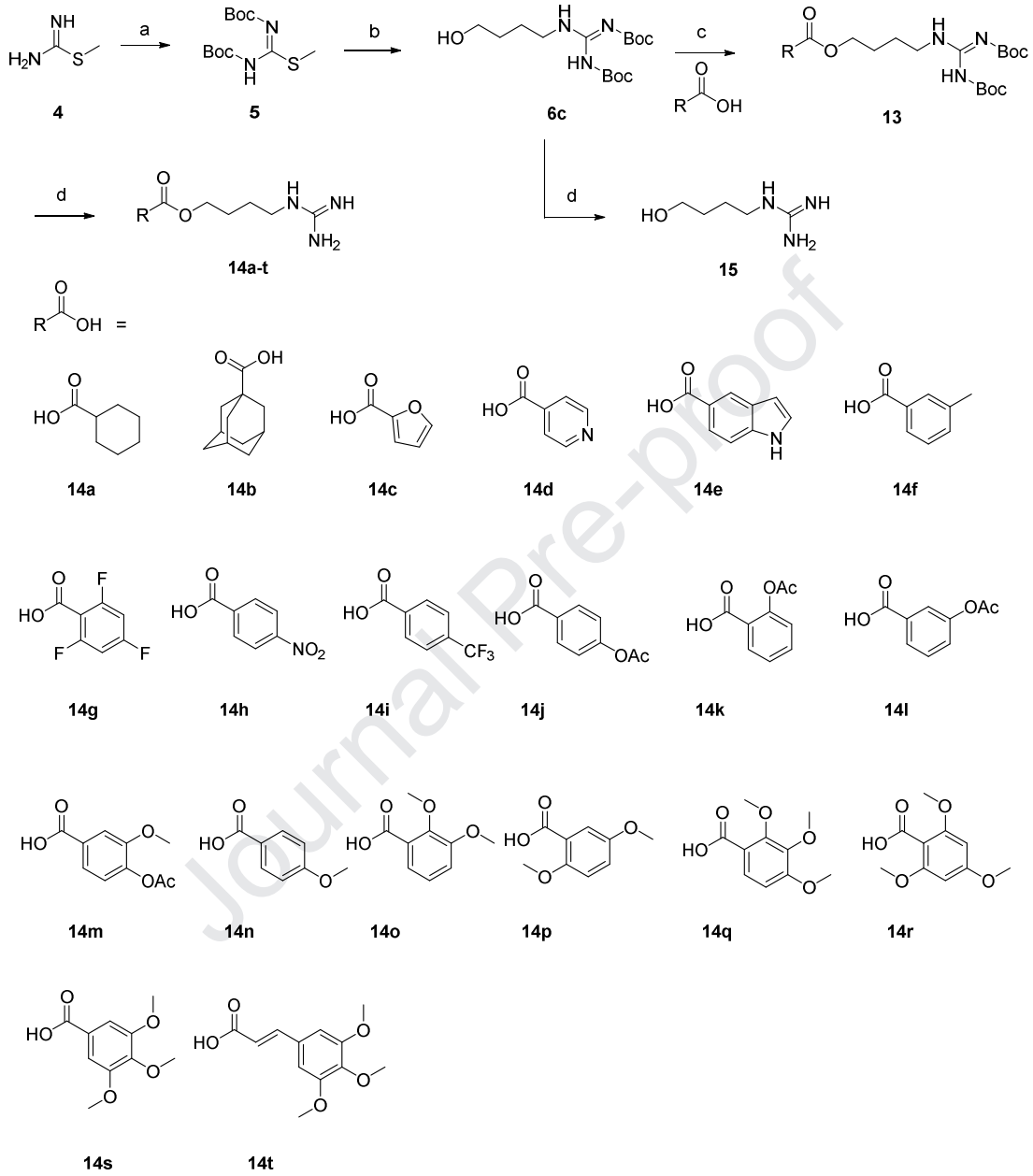

[a]Reagents and conditions: (a) $(Boc)_2O$, $NaHCO_3$, DCM, r.t., 7 d, 96%; (b) 4-Amino-1-butanol, DMF, r.t., 12 h, 99%; (c) EDCI, DMAP, DCM, r.t., 2-18 h, 83-98%; (d) $ZnBr_2$, DCM, r.t., 1-24 h, 78-94%.

Scheme 3. Synthesis of SCM-198 analogs **17a-d** and **19**[a]

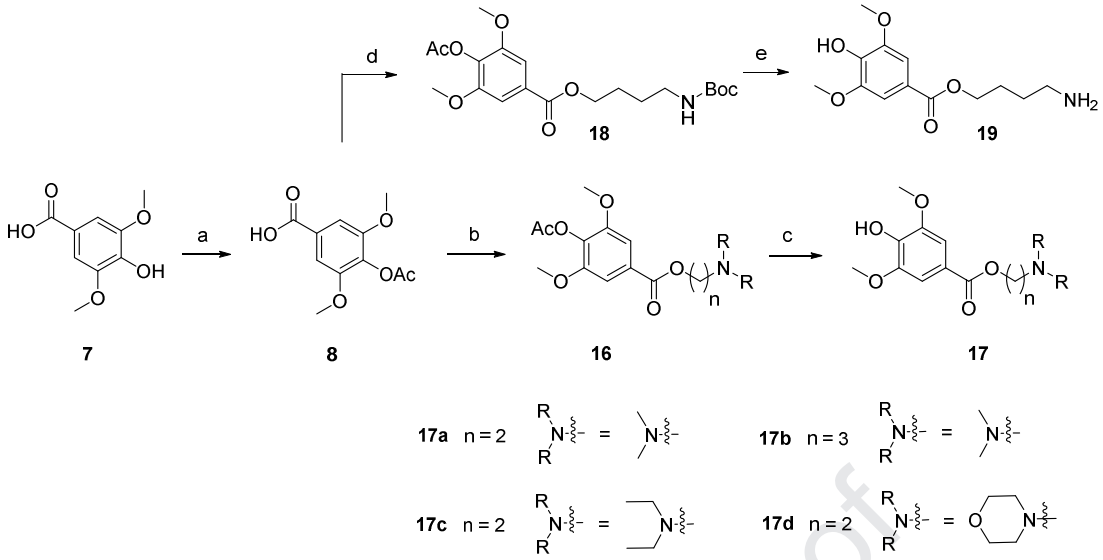

[a]Reagents and conditions: (a) Ac_2O, TEA, DCM, r.t., 5 h, 97%; (b) EDCI, DMAP, DCM, r.t., 4-8 h, 83-98%; (c) NaOH, MeOH, r.t., 5-8 min, 73-91%; (d) EDCI, DMAP, DCM, r.t., 2 h, 94%; (e) NaOH, MeOH, r.t., 5 min, then $ZnBr_2$, DCM, r.t., 12 h, 79%.

2.2 Analysis of Primary Cardiac Myocytes Viability

Oxidative stress is a main cause of cardiomyocyte apoptosis during myocardial infarction. Therapies that reduce reactive oxygen species (ROS) production or increase ROS elimination function have been proved to be beneficial for cardiomyocytes during ischemia [21]. Compared to other oxidative species, such as hydroxyl radicals (•OH), hydrogen peroxide (H_2O_2) is more stable and is believed to play an important role in oxidative stress. Therefore, H_2O_2 is widely used as an oxidant to study oxidative injury in cardiomyocytes [22]. In the current study, the anti-oxidative activities of the newly synthesized compounds were evaluated in a cellular hypoxic model in which oxidative injury was induced by H_2O_2 in cultured H9c2 cells.

H9c2 cells in 96-well plates were treated with 500 nM of H_2O_2, and the cytotoxicity was assayed 1 hour after stimulation *via* MTT assay as the model group. We next evaluated the anti-oxidative effects of the newly synthesized analogs. H9c2 cells were pretreated with compounds (1, 10 μM) for 4 hours, followed by stimulation with H_2O_2 for another 1 hour and the cell viability was determined using

MTT method. Results were showed in Table 1, most of the compounds exhibited more potent anti-oxidative activities at a concentration of 10 μM than 1 μM. Varying the type and the length of the linker suggested that butanolamine (**11c**, namely SCM-198) was a favorable linker after comparing the data of compounds **11a-h**. In addition, compound **11f** considerably protected cells from H_2O_2-induced hypoxic injury and was even more potent at both 1 and 10 μM than SCM-198, implying that introducing non-carbon atoms into the linker might be a preferred option. Compound **15** showed no protective activity, indicating the importance of syringate, and the replacement of syringate with aliphatic acids and heterocyclic acids was also inadvisable (**14a-e**). The bioassay data from aromatic ring substitutions seems to be confusing, but surely the methoxy group at the para-position was unfavorable (**14n**, **14q-t**). The acetyl group on the syringate was adverse to the protective effect of SCM-198 and its analogs, which was proved by compounds **12c** and **12h**. The guanidine of SCM-198 was also important, the removal of guanidine resulted the loose of protective effect (**19**). However, the paradox is some tertiary amines (**17b-c**) can replace the guanidine and exerted potent protective effects comparable to that of SCM-198, which deserved further investigation.

The results of preliminary screening showed that among these tested compounds, four analogs **11f**, **14f**, **14o**, **17c** were the most efficient compounds, which demonstrated increased viability effect than SCM-198 at both 1 and 10 μM concentrations. Thus, the ED_{50} values of these four compounds were further identified using H9c2 cells. H9c2 cells were pretreated with various concentrations of compounds, and ED_{50} were calculated from the relationship between logarithmic value of compound dose and percentage of viability (Table 2). The results showed that compound **14o** was the most potent one with ED_{50} value of 142 ± 3 nM, which was more potent than SCM-198 (192 ± 4 nM).

Table 1. Protective Effects of Compounds on Hypoxia-Induced H9c2 Cells[a]

Compounds	% of viability

	1 μM	10 μM[b]
SCM-198 (**11c**)	52.4 ± 8.1	62.7 ± 6.0*
11a	53.6 ± 8.3	61.9 ± 6.3*
11b	50.1 ± 9.2	55.2 ± 11.2
11d	58.9 ± 2.4	50.1 ± 5.4
11e	53.4 ± 9.2	58.9 ± 6.2*
11f	63.4 ± 5.3*	69.8 ± 4.2*
11g	52.2 ± 10.3	54.2 ± 7.9
11h	56.2 ± 7.3	61.0 ± 8.2*
14a	52.4 ± 1.2	58.8 ± 7.2
14b	58.2 ± 3.7	56.8 ± 5.9
14c	51.1 ± 4.4	53.2 ± 6.2
14d	54.0 ± 9.4	53.2 ± 1.8
14e	51.8 ± 4.8	58.9 ± 4.2*
14f	64.4 ± 8.2*	65.8 ± 9.2*
14g	69.6 ± 9.3*	60.7 ± 5.2*
14h	67.7 ± 8.2*	59.6 ± 7.3*
14i	54.2 ± 3.8	51.7 ± 8.3
14j	57.8 ± 9.0	52.7 ± 7.4
14k	57.8 ± 9.4	58.3 ± 3.0
14l	59.7 ± 6.2*	62.8 ± 5.1*
14m	63.4 ± 3.9*	56.4 ± 8.3
14n	61.2 ± 2.8*	58.6 ± 5.2*
14o	69.3 ± 10.2*	65.3 ± 8.0*
14p	53.3 ± 8.4	57.7 ± 5.3
14q	49.2 ± 7.4	57.8 ± 5.3
14r	55.2 ± 5.3	53.4 ± 9.2
14s	54.1 ± 12.0	53.3 ± 5.7
14t	55.4 ± 5.9	61.4 ± 7.2*

17a	47.8 ± 1.9	48.5 ± 3.7
17b	55.2 ± 4.4	61.7 ± 7.2*
17c	61.1 ± 1.7*	66.8 ± 9.0*
17d	52.3 ± 2.4	50.5 ± 8.4
19	56.3 ± 1.8	56.2 ± 3.9
12c	52.3 ± 3.7	55.2 ± 6.8
12h	42.7 ± 1.9	47.0 ± 3.1
15	46.8 ± 0.7	51.4 ± 4.3
Model	46.3 ± 1.2	

[a] Values are expressed as means ± SEM from six independent experiments.

[b] * $p \leqslant 0.05$ as compared with model group.

Table 2. Protective Effect of Compounds on Hypoxia-Induced H9c2 Cells[a]

Compounds	SCM-198	**11f**	**14f**	**14o**	**17c**
ED_{50} (nM)	192 ± 4	151 ± 6	156 ± 7	142 ± 3	207 ± 6
Viability (%)[b]	55.1 ± 2.4	58.8 ± 3.9	57.4 ± 3.8	62.8 ± 2.3	51.7 ± 3.2

[a] Values are expressed as means ± SEM from three independent experiments. The concentrations used for determining EC_{50} were 0, 0.05, 0.1, 0.5, 1.0, 5.0, 10.0 and 20.0 μM.

[b] Viability levels at the EC_{50} concentrations.

2.3 Levels of LDH and Activity of MnSOD

To exam whether increased viability effect of the compound is due to protection of cells against cell damage or increase in cell proliferation, we measured lactate dehydrogenase (LDH) release as a marker of impaired cellular membrane and injury. Normally, LDH exclusively resides in cytoplasma. In case of cell injury or death, LDH will leak into culture medium from the damaged cytoplasmic membrane. The activity of LDH in culture medium is therefore an indicator of the cell damage [23]. H9c2 cells were pretreated with 10 μM of SCM-198, **11f**, **14f**, **14o** and 1 μM of **14o**, respectively, for 4 hours and then stimulated with H_2O_2 for another 1 hour. After that,

culture medium was collected and the LDH activity was determined using LDH activity assay kit. As shown in Figure 2A, cells treated with **14f** showed comparable LDH leakage with that of SCM-198. Surprisingly, the LDH activity in culture medium of cells treated with 1 μM of **14o** was even lower than that treated with 10 μM SCM-198.

As the first-line anti-oxidative enzyme residing in mitochondrion, MnSOD plays an important role in reducing mitochondrial ROS production. Enhanced MnSOD activity is an adaptive strategy for cells to resist oxidative stress [24]. To determine the severity of oxidative stress, the activity of MnSOD in H9c2 cells subjected with H_2O_2 stimulation was further investigated (Figure 2B). We found that the activity of MnSOD increased rigorously in H9c2 cells after H_2O_2 stimulation. However, SCM-198 or **14o** pretreatment preserved the activity of MnSOD, indicating a reduced mitochondrial oxidative stress.

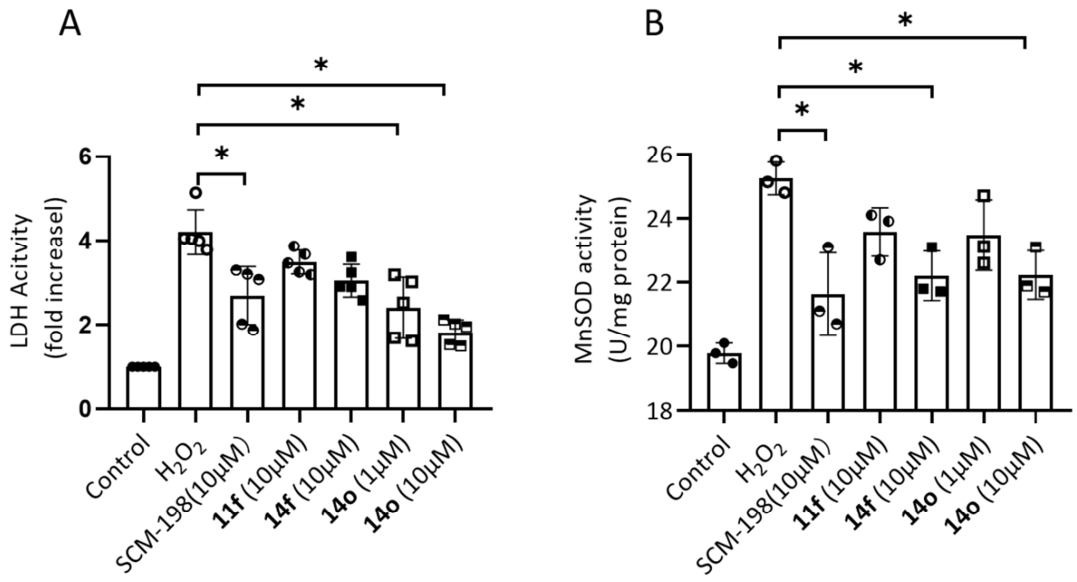

Figure 2. Compound **14o** showed superior anti-oxidative effects than SCM-198 *in vitro*. (A) The release of LDH, a marker of cardiomyocytes injury, was determined in culture medium. **14o** showed comparable cardioprotective effect at 1 μM with SCM-198 at 10 μM. N = 5 for each group. (B) The activity of MnSOD was determined in H9c2 cells treated with different analogs. **14o** (10 μM) and **14f** (10 μM) showed comparable anti-oxidative effects with SCM-198 at 10 μM. N = 3 for each

group, and data were represented as Mean ± SD. * $p \leq 0.05$ as indicated.

2.4 Analysis of Apoptosis-Related Proteins

We further determined the expression of apoptosis related proteins in H9c2 cells treated with these compounds. The onco-protein Bcl-2 resides at the outer membrane of mitochondrion and plays important roles in mitochondrial redox regulation. In hypoxic condition, Bcl-2 implicated in reducing mitochondrial apoptosis by inhibiting the opening of mitochondrial permeability transition pore (MPTP) and reducing the release of cytochrome c. There is also evidence that Bcl-2 participates in regulation of mitochondrial ROS production [25]. Therefore, in addition to be a marker of cell apoptosis, Bcl-2 level is also related to the function and ROS production of mitochondrion. Thus, the Bcl-2 expression level was tested in H9c2 cells pretreated with 10 μM SCM-198, **11f**, **14f** and 1 μM **14o**, respectively. Bcl-2 levels were significantly reduced after H_2O_2 stimulation, and SCM-198 pretreatment restored it to about 50% of the control group (Figure 3A). Analog **14o** comparably increased Bcl-2 level at the concentration of 1 μM, while **11f** at the concentration of 10 μM, showed little benefit on the level of Bcl-2.

Caspases are a series of apoptosis operating enzymes responsible for degrading multiple functional proteins during cell apoptosis. It is believed to be downstream effectors of Bcl-2 family [26]. We then tested the activation of caspase 3 in different treatment groups, and found that H_2O_2 could significantly increase level of cleaved-caspase 3, both SCM-198 (10 μM) and **14o** (1 μM) were able to impede the activation of caspase 3 in cells subjected with H_2O_2 stimulation (Figure 3B).

In summary, the above results revealed that analog **14o** might be a potential cardio-protective agent with higher efficiency than SCM-198.

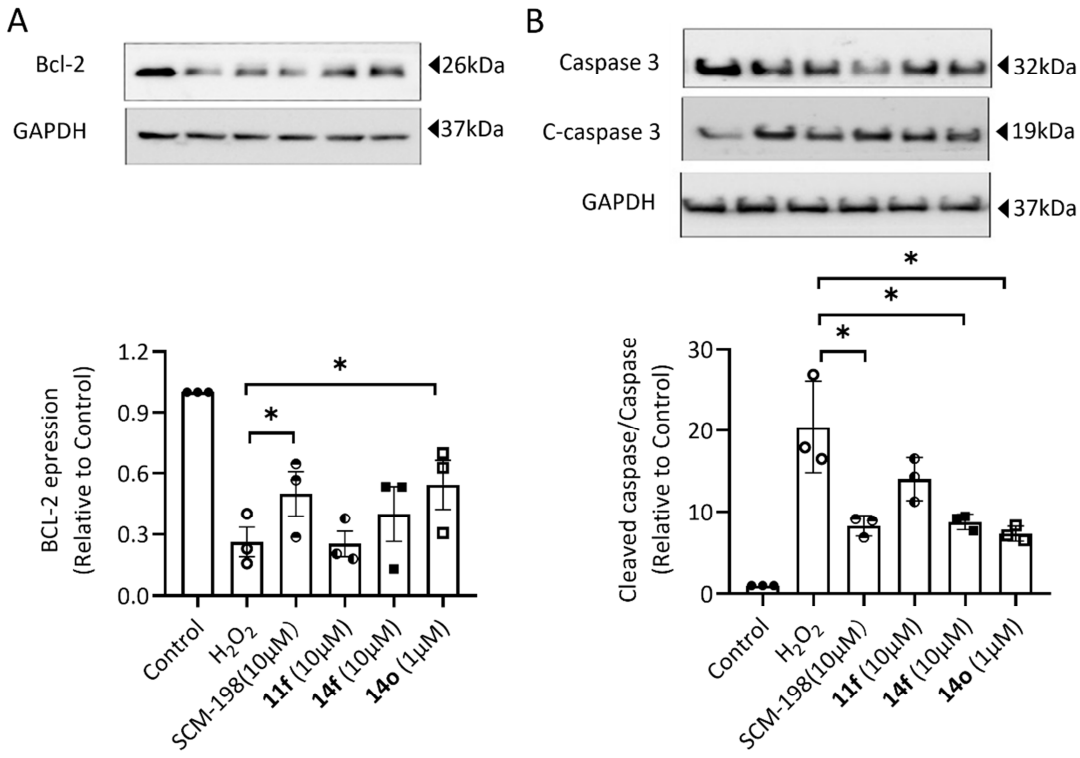

Figure 3. Compound **14o** showed superior anti-apoptotic effects than SCM-198 *in vitro*. H9c2 cells were pretreated with SCM-198 (10 μM), **11f** (10 μM), **14f** (10 μM) and **14o** (1 μM) for 4 hours, followed by stimulation with H_2O_2 for another 1 hour, and the level of (A) Bcl-2 and (B) cleaved caspase 3 (C-caspase 3) were determined by western blotting. The lower panels were statistical results of Bcl-2 and C-caspase 3/Caspase 3. N = 3 for each group, and data were represented as Mean±SD. *$p \leq 0.05$ as indicated.

*2.5 Compound **14o** Attenuated H_2O_2-Induced Reduction of Mitochondrial Membrane Potential*

In order to further understand the cardio-protective mechanism of these SCM-198 analogs, the most effective compound **14o** was selected to explore its mechanism of action. According to the above results, compound **14o** obviously restored the level of Bcl-2 in hypoxia, indicating that it might reduce ROS production or mitochondrial injury. H_2O_2 caused a variety of cellular dysfunctions mainly through dissipation of electrical potential gradient across the inner membrane of mitochondria. Changes in

the mitochondrial membrane potential (Δψm) have been postulated to be early events in H_2O_2-induced apoptosis signaling pathway [27]. Fluorescent probe JC-1 was used to measure the changes of Δψm. JC-1 can selectively enter into mitochondria and form complexes with intense red fluorescence in healthy cells, however, in unhealthy cells with low Δψm, JC-1 remains in the monomeric form, which displays only green fluorescence. As shown in Figure 4A, in healthy cells, JC-1 aggregated in mitochondria and showed as red dots under fluorescent microscope. H_2O_2 incubation caused apoptosis of cells and after JC-1 was loaded, only few cells showed orange fluorescent while most of the cells showed green fluorescence, indicating disperse of Δψm. SCM-198 pretreatment impeded this Δψm loss indicated by the increased red fluorescence and the **14o** pretreatment protected mitochondria from injury more effectively. These findings further confirmed that **14o** reduced cell apoptosis and preserved mitochondrial membrane potential.

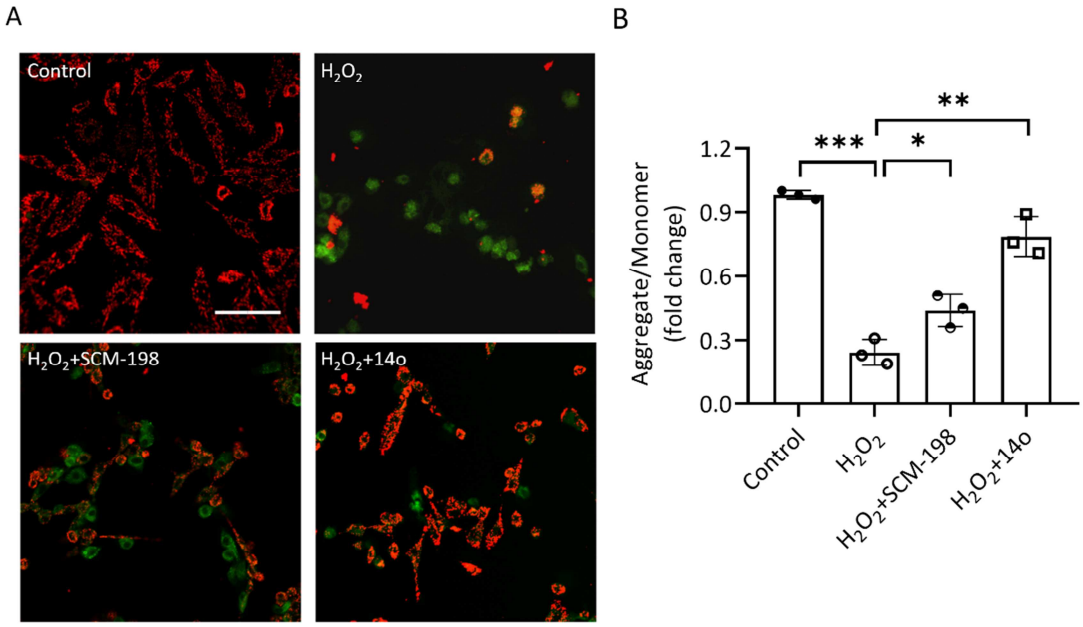

Figure 4. Compound **14o** showed better protective effects on Δψm than SCM-198. H9c2 cells were pretreated with SCM-198 (10 μM) and **14o** (1 μM) for 4 hours, followed by stimulation with H_2O_2 for another 1 hour, H9c2 cells were then incubated with JC-1 for 30 min to determine the Δψm. (A) Representative images of JC-1 staining in different treatment groups. Red fluorescence indicated healthy mitochondria with high membrane potential, while green fluorescence indicated

injured mitochondria with reduced membrane potential. Scale bar: 10 μm. (B) Quantification of $\Delta\psi$m was expressed as a ratio between monomer and aggregate fluorescence (Red/Green) of three independent fields from each group, and data were represented as Mean ± SD. *$p \leq 0.05$, **$p \leq 0.01$, ***$p \leq 0.001$ as indicated.

*2.6 In vivo Cardioprotective Effects of **14o***

After confirming the *in vitro* activity of **14o**, we further detected its *in vivo* cardio-protective effects in a mouse model of AMI with SCM-198 as the positive control. Mice were intraperitoneally injected with SCM-198 at a dose of 10 mg/kg/day, as determined in our previous work [28], or injected with **14o** at a dose of 5 mg/kg/day, for 7 consecutive days, before subjected to AMI. During this period, no obvious changes including diarrhea and loss of body weight could be observed, suggesting the low toxicity of **14o**. Then, AMI was induced by permanent ligation of left anterior descending (LAD) coronary artery in C57BL/6J mice and the infarct size was determined by 2,3,5-triphenyltetrazolium chloride (TTC) staining. As indicated in Figure 5A, LAD induced severe infarction in left ventricle (pale area), and administration of SCM-198 remarkably reduced the infarct size. Notably, compared with SCM-198, mice in **14o** treatment group had much lower cardiac infarct size (Figure 5B). H&E staining was further used to evaluate the histological features of the infarcted hearts. The results in Figure 5C showed that in AMI group, myofilaments condensed in peri-infarct heart, leaving a damaged gap junction with infiltrated nuclei from necrotic or apoptotic cardiomyocytes. Compound **14o** significantly reduced the damage within the epimyocardium and alleviated the morphological damage of cardiomyocytes. These *in vivo* results indicated that **14o** was a preferable candidate for the treatment of AMI.

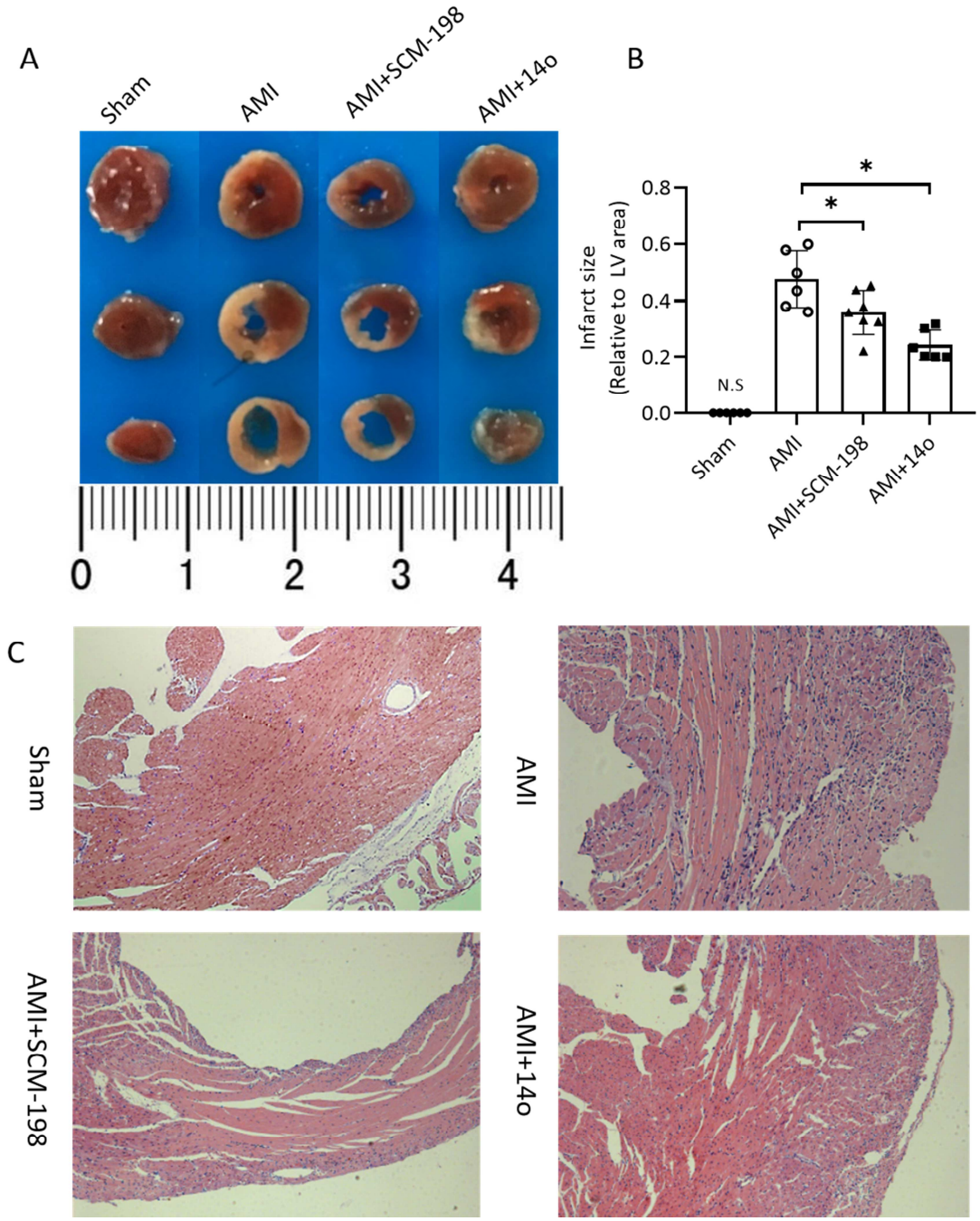

Figure 5. Compound **14o** (5 mg/kg/day) reduced the infarct size in mice subjected with AMI. (A) Heart of mice in SCM-198, **14o** and saline-treated (Sham) groups were sectioned and stained with TTC for 30 min, viable myocardium was stained with red and infarct myocardium was pale. (B) Quantifications of infarct size determined as percentage of left ventricular (LV) area, N = 6 for Sham, AMI, and AMI+**14o** group, N = 7 for AMI+SCM-198 group. *$p \leq 0.05$ as indicated. (C) H&E staining was performed using heart sections to determine the morphological changes.

*2.7 Analog **14o** Reduced Apoptosis of Cardiomyocytes in Mice Subjected with AMI*

Cardiomyocytes apoptosis accounts for 70-80% of cell death after myocardial infarction. After ischemic injury, cells in the area at risk (AAR) are in deficiency of both blood and oxygen and are most likely to be injured. Therefore, reducing apoptosis of cardiomyocytes in AAR is of great significance for reducing infarct size [29]. The *in vitro* studies confirmed the anti-apoptotic activity of compound **14o**, in order to determine whether **14o** could reduce apoptosis of cardiomyocytes in AAR *in vivo*, TUNEL staining was applied to detect the apoptosis. DNA fragmentation that results from apoptosis can be labeled with a fluorescent marker. As shown in Figure 6A, TUNEL positive staining cells were hardly found in cardiac section of sham operated mice, while massive red fluorescent dots in peri-infarct area indicating fragments of DNA were observed in model group. As expected, SCM-198 and **14o** obviously reduced the number of TUNEL-positive cells in peri-infarct area. Statistical results indicated that the number of apoptotic cells in SCM-198 and **14o** treated mice was significantly (p<0.05) lower than that in AMIC mice (Figure 6B). Moreover, the efficiency of **14o** was much higher than that of SCM-198. Accordingly, the above *in vivo* results indicated that compound **14o** reduced myocardial infarction-induced apoptosis of cardiomyocytes.

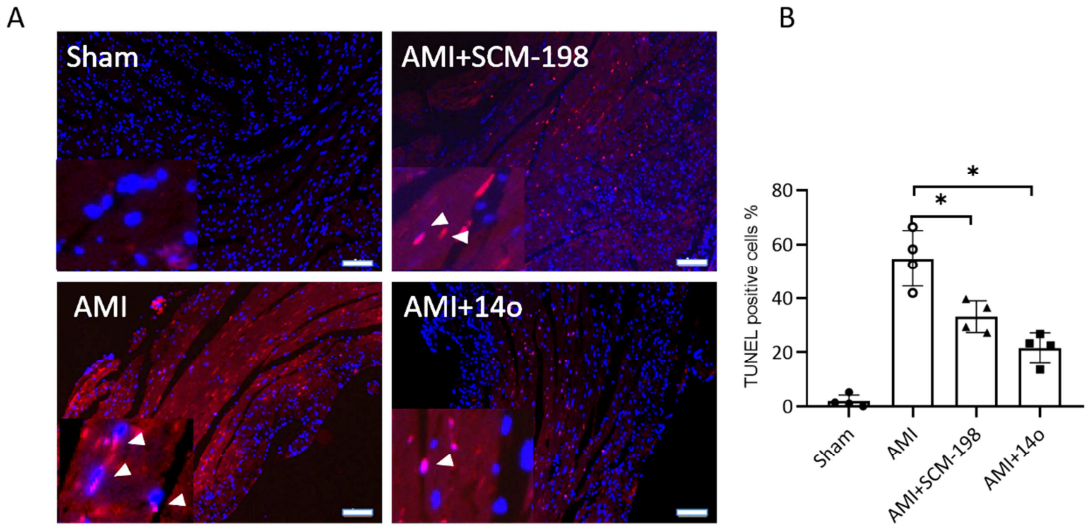

Figure 6. Compound **14o** at 5 mg/kg/day reduced apoptosis of cardiomyocytes in mice subjected to AMI. (A) Immunostaining for apoptotic cardiomyocytes in border

areas of SCM-198, **14o** or saline-treated mice. High magnifications of the apoptotic cells have been shown at the corner of each illustration. Apoptotic cells were indicated with white arrowhead. (B) Quantifications of TUNEL positive staining (red dots) determined as percentage of DAPI-positive nucleus (blue dots). Scale bars = 250 μm, N = 4 for each group, *$p \leq 0.05$ as indicated.

*2.8 Pharmacokinetic Profiles of **14o***

Previous pharmacokinetic studies of SCM-198 showed that it has a quick metabolism with a half-life of about 2 h and poor oral bioavailability (1.78%) [30]. A pharmacokinetic evaluation of compound **14o** was conducted after intravenous (i.v.) and oral (i.g.) dosing in male Sprague-Dawley rats (N = 3 per dose route). As illustrated in Table 3, following i.v. dosing with 1 mg/kg in fasted animals, compound **14o** has a terminal elimination half-life ($t_{1/2}$) of 1.67 h with a volume of distribution and total body clearance of 3766 mL/kg and 1592 mL/min/kg, respectively. The oral bioavailability of compound **14o** (10 mg/kg, i.g.) was 18.5%, which was much higher than SCM-198. In addition, the residence time of **14o** is longer than SCM-198, with a $t_{1/2}$ of 4.87 h. The structure comparison of **14o** and SCM-198 implied that the improvement of pharmacokinetic profiles of **14o** might be attributed to the removal of phenol group, which is a labile site susceptible to metabolic glucuronidation [31].

Table 3. The Main Pharmacokinetic Parameters of Compound 14o (Mean ± SD, N = 3)

Route Dose (mg/kg)	AUC_{last} (ng·h/mL)	AUC_{inf} (ng·h/mL)	C_{max} (ng/mL)	$t_{1/2}$ (h)	Cl_F_obs (mL/min/kg)	Vz_F_obs (mL/kg)	*F* (%)
i.v. (1)	882 ± 143	895 ± 121	764 ± 184	1.63 ± 0.47	1592 ± 432	3766 ± 257	-
i.g. (10)	1634 ± 261	1680 ± 210	621 ± 159	4.87 ± 0.83	5573 ± 737	43706 ± 2650	18.5%

3. Conclusion

A series of SCM-198 analogs were synthesized by replacing the aromatic ring, linker, and guanidine moieties of SCM-198 separately for the first time, and the cardioprotective effects of these analogs were also evaluated. The SARs studies implied that butanolamine and guanidine were vital for the cardioprotective effects of SCM-198 and the aromatic ring tolerated various substituents. Three analogs (**11f**, **14f**, and **14o**) with higher anti-apoptotic potency than SCM-198 were identified as determined by MTT cell viability assay and confirmed by LDH leakage on H9c2 cells challenged with H_2O_2. Further mechanism studies indicated that these compounds could preserve the activity of MnSOD and the most potent compound **14o** impeded the dissipation of $\Delta\psi m$ as well as partly restored the expression of Bcl-2 and reduced the activation of casepase-3. The *in vivo* experiment on MI mouse model indicated that **14o** could significantly reduce infarct size and apoptosis of cardiomyocytes in AAR, as determined by TTC and TUNEL staining. Moreover, the metabolism and bioavailability of **14o** is promising and much better than SCM-198.

Overall, the most potent analog **14o**, which prominently reduced cardiomyocytes apoptosis and alleviated myocardial infarction induced by coronary ligation, might serve as a potential cardioprotective agent for the treatment of acute myocardial infarction.

4. Experimental section

4.1 Chemistry

4.1.1 General information

All commercially available reagents were used without further purification. Anhydrous solvents were dried through routine protocols. Flash column chromatography was carried out on 200-300 mesh silica gel (Qingdao Haiyang Chemical, China). Reactions were monitored by thin-layer chromatography (TLC) on 0.25 mm silicagel plates (GF254) and visualized under UV light. ^{1}H NMR and ^{13}C NMR spectra were recorded with a Bruker AV-300 spectrometer (Bruker Company, Germany) in the indicated solvents ($CDCl_3$ or DMSO-d_6, TMS as internal standard): the values of the chemical shifts are expressed in δ values (ppm) and the coupling

constants (*J*) in Hz. Low-and high-resolution mass spectrums (LRMS and HRMS) were measured on Finnigan MAT 95 spectrometer (Finnigan, Germany). Melting points were recorded with Buchi melting point apparatus and are uncorrected. Flash column chromatography was carried out on 200-300 mesh silica gel purchased from Qingdao Haiyang Chemical Co., Ltd.

*4.1.2 Procedure for the Synthesis of Intermediates **5**, **6**, **9**.*

The intermediates **5**, **6**, and **9** were prepared according to our previous procedure and used for the next step without purification except for compounds **9c** and **9h**, which were purified by silica gel column chromatography (EtOAc/petroleum ether, 2:1) to get the compounds as white solids (Yield 95%).[15,18]

4.1.2.1

*4-(2,3-Bis(tert-butoxycarbonyl)guanidino)butyl-4-acetoxy-3,5-dimethoxybenzoate (**9c**).*

Yield 95%, white solid, m.p. 97~99^{o}C. ^{1}H NMR ($CDCl_3$, 300 MHz): δ (ppm) 11.51 (s, 1H), 8.38 (s, 1H), 7.32 (s, 2H), 4.36 (m, 2H), 3.88 (s, 6H), 3.53 (m, 2H), 2.35 (s, 3H), 1.82 (m, 4H), 1.50 (s, 9H), 1.49 (s, 9H); ^{13}C NMR ($CDCl_3$, 75 MHz): δ (ppm) 168.2, 165.9, 163.6, 156.2, 153.3, 152.1, 128.2, 106.3, 83.2, 79.3, 64.8, 56.3, 40.4, 28.3, 28.0, 26.2, 25.8, 20.4; MS (ESI) *m/z*: 354.4 $[M\text{-}2Boc+H]^{+}$.

4.1.2.2

*(1-(N,N'-bis(tert-butoxycarbonyl)carbamimidoyl)piperidin-4-yl)methyl-4-acetoxy-3,5-dimethoxybenzoate (**9h**).*

Yield 95%, white solid, m.p. 128~130^{o}C. ^{1}H NMR ($CDCl_3$, 300 MHz): δ (ppm) 10.19 (br, 1H), 7.29 (s, 2H), 4.22 (m, 4H), 3.88 (s, 6H), 2.97 (t, 2H), 2.35 (s, 3H), 2.05 (m, 1H), 1.82 (m, 2H), 1.51 (m, 2H), 1.50 (s, 9H), 1.49 (s, 9H); ^{13}C NMR ($CDCl_3$, 75 MHz): δ (ppm) 168.2, 165.7, 155.1, 152.1, 128.1, 106.3, 68.8, 56.3, 35.6, 28.6, 28.1, 20.4; MS (ESI) *m/z*: 480.3 $[M\text{-}Boc+H]^{+}$.

*4.1.3 Procedure for the Synthesis of Intermediates **10a-10h**.*

To the solution of **9a-9h** in anhydrous methanol, NaOH (1 equiv) was added and stirred at room temperature for 5-10 min. Concentration to dryness afforded crude products which were purified by silica gel column chromatography (EtOAc/petroleum ether,

4:1) to provide **10a-10h** as white solids (Yield 82-90%).

4.1.3.1

*2-(2,3-Bis(tert-butoxycarbonyl)guanidino)ethyl-4-hydroxy-3,5-dimethoxybenzoate (**10a**).*

Yield 84%, white solid, m.p. 81~85°C. ^{1}H NMR ($CDCl_3$, 300 MHz): δ (ppm) 11.54 (br, 1H), 8.77 (s, 1H), 7.36 (s, 2H), 6.01 (br, 1H), 4.43 (t, J = 5.1 Hz, 2H), 3.96 (s, 6H), 3.86 (m, 2H), 1.51 (s, 9H), 1.48 (s, 9H); ^{13}C NMR ($CDCl_3$, 75 MHz): δ (ppm) 165.9, 163.4, 156.3, 153.2, 146.7, 139.4, 120.7, 106.7, 83.1, 79.5, 63.1, 56.4, 39.7, 28.2, 28.0; MS (ESI) *m/z*: 284.2 $[M\text{-}2Boc+H]^+$.

4.1.3.2

*3-(2,3-Bis(tert-butoxycarbonyl)guanidino)propyl-4-hydroxy-3,5-dimethoxybenzoate (**10b**).*

Yield 82%, white solid, m.p. 88~90°C. ^{1}H NMR ($CDCl_3$, 300 MHz): δ (ppm) 11.40 (br, 1H), 8.43 (s, 1H), 7.24 (s, 2H), 5.99 (br, 1H), 4.33 (t, J = 6.0 Hz, 2H), 3.86 (s, 6H), 3.53 (m, 2H), 2.00 (m, 2H), 1.42 (s, 9H), 1.41 (s, 9H); ^{13}C NMR ($CDCl_3$, 75 MHz): δ (ppm) 165.8, 163.1, 155.7, 152.7, 146.1, 138.9, 120.4, 106.2, 82.7, 78.9, 62.0, 55.9, 37.6, 27.7, 27.6, 27.5; MS (ESI) *m/z*: 298.3 $[M\text{-}2Boc+H]^+$.

4.1.3.3

*4-(2,3-Bis(tert-butoxycarbonyl)guanidino)butyl-4-hydroxy-3,5-dimethoxybenzoate (**10c**).*

Yield 83%, white solid, m.p. 85~88°C. ^{1}H NMR (DMSO-d_6, 300 MHz): δ (ppm) 11.51 (s, 1H), 8.36 (s, 1H), 7.26 (s, 2H), 6.05 (br, 1H), 4.31 (m, 2H), 3.86 (s, 6H), 3.45 (s, 1H), 1.76 (m, 4H), 1.46 (s, 9H), 1.44 (s, 9H); ^{13}C NMR (DMSO-d_6, 75 MHz): δ (ppm) 174.3, 165.8, 163.0, 155.2, 152.0, 147.8, 106.8, 82.8, 78.0, 63.7, 55.8, 27.9, 27.5, 25.7, 25.3, 23.6; MS (ESI) *m/z*: 311.3 $[M\text{-}2Boc+H]^+$.

4.1.3.4

*5-(2,3-Bis(tert-butoxycarbonyl)guanidino)pentyl-4-hydroxy-3,5-dimethoxybenzoate (**10d**).*

Yield 90%, white solid, m.p. 84~86°C. ^{1}H NMR ($CDCl_3$, 300 MHz): δ (ppm) 11.52 (br, 1H), 8.34 (s, 1H), 7.29 (s, 2H), 6.00 (br, 1H), 4.29 (t, J = 6.0 Hz, 2H), 3.92 (s, 6H), 3.44

(m, 2H), 1.79 (m, 2H), 1.63 (m, 2H), 1.50 (m, 2H), 1.48 (s, 9H), 1.47 (s, 9H); ^{13}C NMR ($CDCl_3$, 75 MHz): δ (ppm) 165.9, 155.6, 152.8, 146.1, 138.7, 120.7, 106.1, 82.7, 78.9, 64.2, 55.9, 40.3, 28.2, 27.9, 27.8, 27.5, 22.9; MS (ESI) *m/z*: 326.3 $[M\text{-}2Boc+H]^+$.

4.1.3.5

*6-(2,3-Bis(tert-butoxycarbonyl)guanidino)hexyl-4-hydroxy-3,5-dimethoxybenzoate (**10e**).*

Yield 88%, white solid, m.p. 82~84^{o}C. ^{1}H NMR ($CDCl_3$, 300 MHz): δ (ppm) 11.43 (br, 1H), 8.27 (s, 1H), 7.24 (s, 2H), 5.99 (br, 1H), 4.22 (t, J = 6.0 Hz, 2H), 3.87 (s, 6H), 3.36 (m, 2H), 1.70 (m, 2H), 1.53 (m, 2H), 1.51 (m, 4H), 1.42 (s, 9H), 1.41 (s, 9H); ^{13}C NMR ($CDCl_3$, 75 MHz): δ (ppm) 165.9, 163.2, 155.5, 152.8, 146.1, 138.7, 120.9, 106.1, 82.7, 78.9, 64.4, 55.9, 40.4, 28.4, 28.2, 27.8, 27.5, 26.0, 25.2; MS (ESI) *m/z*: 340.4 $[M\text{-}2Boc+H]^+$.

4.1.3.6

*6-((tert-Butoxycarbonyl)amino)-2,2-dimethyl-4-oxo-3,10-dioxa-5,7-diazadodec-5-en-12-yl 4-hydroxy-3,5-dimethoxybenzoate (**10f**).*

Yield 90%, white solid, m.p. 81~83^{o}C. ^{1}H NMR ($CDCl_3$, 300 MHz): δ (ppm) 11.44 (br, 1H), 8.62 (s, 1H), 7.32 (s, 2H), 5.89 (br, 1H), 4.46 (t, J = 5.7 Hz, 2H), 3.93 (s, 6H), 3.83 (t, J = 5.7 Hz, 2H), 3.62 (m, 4H), 1.48 (s, 9H), 1.47 (s, 9H); ^{13}C NMR ($CDCl_3$, 75 MHz): δ (ppm) 166.3, 163.5, 156.3, 153.0, 146.6, 106.8, 83.0, 79.3, 72.4, 69.4, 69.0, 64.0, 61.8, 56.4, 40.6, 28.2, 28.0, 27.9; MS (ESI) *m/z*: 328.6 $[M\text{-}2Boc+H]^+$.

4.1.3.7

*1-(2,3-Bis(tert-butoxycarbonyl)guanidino)propan-2-yl-4-hydroxy-3,5-dimethoxybenzoate (**10g**).*

Yield 88%, white solid, m.p. 70~72^{o}C. ^{1}H NMR ($CDCl_3$, 300 MHz): δ (ppm) 11.52 (br, 1H), 8.73 (s, 1H), 7.33 (s, 2H), 5.27 (s, 1H), 3.95 (s, 6H), 3.72 (m, 3H), 1.50 (s, 9H), 1.45 (s, 9H), 1.40 (m, 3H); ^{13}C NMR ($CDCl_3$, 75 MHz): δ (ppm) 165.6, 163.5, 156.6, 153.2, 146.6, 139.3, 106.7, 83.1, 79.4, 69.8, 56.4, 44.9, 28.2, 27.9, 17.6; MS (ESI) *m/z*: 298.2 $[M\text{-}2Boc+H]^+$.

4.1.3.8

(1-(N,N'-bis(tert-butoxycarbonyl)carbamimidoyl)piperidin-4-yl)methyl-4-hydroxy-3,5

*-dimethoxybenzoate (**10h**).*

Yield 82%, white solid, m.p. 102~103°C. ^{1}H NMR (DMSO-d_6, 300 MHz): δ (ppm) 9.52 (br, 1H), 7.20 (s, 2H), 4.11 (d, J = 6.0 Hz, 2H), 4.01 (m, 2H), 3.80 (s, 6H), 3.21 (m, 1H), 2.84 (t, J = 6.0 Hz, 2H), 1.74 (m, 2H), 1.37 (s, 18H), 1.19 (m, 2H); ^{13}C NMR ($CDCl_3$, 75 MHz): δ (ppm) 165.5, 150.9, 147.5, 140.9, 119.1, 106.8, 67.9, 56.0, 45.3, 34.9, 28.0, 27.9; MS (ESI) *m/z*: 338.3 $[M-2Boc+H]^+$.

*4.1.4 Procedure for the Synthesis of Compounds **11a-11h**.*

Compounds **10a-10h** (1 equiv, 0.41 mmol) and zinc bromide (5 equiv, 2.1 mmol) were stirred in DCM at r.t. for 1-12 h. Then, the crude products were purified by flash chromatography using DCM/MeOH 10:1 (v/v) as eluent, furnish **11a-11h** as white solids (71-95%).

*4.1.4.1 2-Guanidinoethyl-4-hydroxy-3,5-dimethoxybenzoate (**11a**).*

Yield 92%, white solid, m.p. 124~128°C. ^{1}H NMR (DMSO-d_6, 300 MHz): δ (ppm) 9.37 (s, 1H), 7.55 (t, J = 3.6 Hz, 1H), 7.22, (s, 2H), 6.25-7.50 (br, 3H), 4.27 (t, J = 3.6 Hz, 2H), 3.80 (s, 6H), 3.26 (m, 2H); ^{13}C NMR (DMSO-d_6, 75 MHz): δ (ppm) 165.9, 157.4, 148.0, 141.3, 119.4, 107.5, 63.4, 56.6, 49.1; MS (ESI) *m/z*: 284.3 $[M+H]^+$.

*4.1.4.2 3-Guanidinopropyl-4-hydroxy-3,5-dimethoxybenzoate (**11b**).*

Yield 91%, white solid, m.p. 116~118°C. ^{1}H NMR (DMSO-d_6, 300 MHz): δ (ppm) 9.39 (s, 1H), 7.51 (m, 1H), 7.21 (s, 2H), 6.75-7.25 (br, 3H), 4.26 (t, J = 6.0 Hz, 2H), 3.81 (s, 6H), 3.17 (m, 2H), 1.92 (m, 2H); ^{13}C NMR (DMSO-d_6, 75 MHz): δ (ppm) 165.2, 156.6, 147.5, 141.0, 118.6, 106.8, 61.7, 56.1, 49.1, 37.8; MS (ESI) *m/z*: 298.2 $[M+H]^+$.

*4.1.4.3 4-Guanidinobutyl-4-hydroxy-3,5-dimethoxybenzoate (**11c**).*

Yield 93%, white solid, m.p. 106~110°C. ^{1}H NMR (DMSO-d_6, 300 MHz): δ (ppm) 9.35 (s, 1H), 7.44 (m, 1H), 7.20 (s, 2H), 6.75-7.00 (br, 3H), 4.26 (t, J = 6.0 Hz, 2H), 3.81 (s, 6H), 3.17 (m, 2H), 1.72 (m, 2H), 1.58 (m, 2H); ^{13}C NMR (DMSO-d_6, 75 MHz): δ (ppm) 166.1, 157.1, 148.0, 141.2, 119.8, 107.2, 70.2, 64.4, 56.6, 49.1, 26.0, 25.7; MS (ESI) *m/z*: 312.1 $[M+H]^+$.

*4.1.4.4 5-Guanidinopentyl-4-hydroxy-3,5-dimethoxybenzoate (**11d**).*

Yield 95%, white solid, m.p. 104-106°C. ^{1}H NMR (DMSO-d_6, 300 MHz): δ (ppm) 9.34

(s, 1H), 7.44 (m, 1H), 7.21 (s, 2H), 6.75-7.25 (br, 3H), 4.26 (t, J = 6.0 Hz, 2H), 3.89 (s, 6H), 3.23 (m, 2H), 1.72 (m, 2H), 1.63 (m, 2H), 1.58 (m, 2H); ^{13}C NMR (DMSO-d_6, 75 MHz): δ (ppm) 165.3, 157.4, 148.1, 141.7, 119.9, 107.1, 64.8, 56.1, 40.1, 26.0, 25.8; MS (ESI) *m/z*: 326.2 $[M+H]^+$.

*4.1.4.5 6-Guanidinohexyl-4-hydroxy-3,5-dimethoxybenzoate (**11e**).*

Yield 92%, white solid, m.p. 104^{o}C. ^{1}H NMR (DMSO-d_6, 300 MHz): δ (ppm) 9.37 (s, 1H), 7.46 (m, 1H), 7.21 (s, 2H), 6.75-7.05 (br, 3H), 4.28 (t, J = 6.0 Hz, 2H), 3.82 (s, 6H), 3.18 (m, 2H), 1.78 (m, 2H), 1.62 (m, 2H), 1.58 (m, 4H); ^{13}C NMR (DMSO-d_6, 75 MHz): δ (ppm) 165.9, 156.8, 147.2, 141.0, 119.5, 107.1, 64.2, 56.1, 48.9, 27.6, 26.0, 25.2; MS (ESI) *m/z*: 340.2 $[M+H]^+$.

*4.1.4.6 2-(2-Guanidinoethoxy)-ethyl-4-hydroxy-3,5-dimethoxybenzoate (**11f**).*

Yield 79%, white solid, m.p. 104~105^{o}C. ^{1}H NMR (DMSO-d_6, 300 MHz): δ (ppm) 9.37 (s, 1H), 7.51 (m, 1H), 7.21 (s, 2H), 6.75-7.25 (br, 3H), 4.36 (t, J = 6.0 Hz, 2H), 3.81 (s, 6H), 3.76 (m, 2H), 3.56 (m, 2H), 3.32 (m, 2H); ^{13}C NMR (DMSO-d_6, 75 MHz): δ (ppm) 165.6, 156.9, 147.5, 140.8, 119.1, 106.8, 68.5, 68.4, 63.7, 56.1, 40.8; MS (ESI) *m/z*: 328.2 $[M+H]^+$.

*4.1.4.7 1-Guanidinopropan-2-yl-4-hydroxy-3,5-dimethoxybenzoate (**11g**).*

Yield 82%, white solid, m.p. 140~142^{o}C. ^{1}H NMR (DMSO-d_6, 300 MHz): δ (ppm) 9.41 (s, 1H), 7.66 (m, 1H), 7.26 (s, 2H), 6.75-7.45 (br, 3H), 5.10 (s, 1H), 3.84 (s, 6H), 3.42 (m, 2H), 1.31 (m, 3H); ^{13}C NMR (DMSO-d_6, 75 MHz): δ (ppm) 165.9, 158.2, 146.8, 140.1, 106.8, 83.1, 56.5, 44.8, 17.4; MS (ESI) *m/z*: 298.1 $[M+H]^+$.

*4.1.4.8 (1-Carbamimidoylpiperidin-4-yl)-methyl-4-hydroxy-3,5-dimethoxybenzoate (**11h**).*

Yield 71%, white solid, m.p. >200^{o}C. ^{1}H NMR (DMSO-d_6, 300 MHz): δ (ppm) 9.39 (s, 1H), 7.24 (s, 2H), 6.75-7.25 (br, 3H), 4.14 (m, 2H), 4.04 (m, 2H), 3.84 (s, 6H), 2.88 (t, J = 6.0 Hz, 2H), 2.03 (m, 1H), 1.76 (m, 2H), 1.19 (m, 2H); ^{13}C NMR (DMSO-d_6, 75 MHz): δ (ppm) 165.2, 158.2, 147.9, 141.1, 119.8, 106.6, 67.2, 56.1, 45.4, 34.1, 26.8; MS (ESI) *m/z*: 338.1 $[M+H]^+$.

*4.1.5 Procedure for the Synthesis of Compounds **12c** and **12h**.*

Compounds **9c** and **9h** (1 equiv, 0.41 mmol) and zinc bromide (5 equiv, 2.1 mmol) were

stirred in DCM at r.t. for 4 h. Then, the crude products were purified by flash chromatography using DCM/MeOH 20:1 (v/v) as eluent, furnish **12c** and **12h** as white solids (83-88%).

*4.1.5.1 4-Guanidinobutyl-4-acetoxy-3,5-dimethoxybenzoate (**12c**).*

Yield 88%, white solid, m.p. 138~140^{o}C. ^{1}H NMR ($CDCl_3$, 300 MHz): δ (ppm) 7.45 (m, 1H), 6.29 (s, 2H), 6.75-7.25 (br, 3H), 4.32 (t, J = 6.1 Hz, 2H), 3.81 (s, 6H), 3.30 (m, 2H), 2.28 (s, 3H), 2.20 (s, 6H), 1.72 (m, 2H), 1.62 (m, 2H); ^{13}C NMR ($CDCl_3$, 75 MHz): δ (ppm) 168.2, 165.6, 156.5, 152.3, 132.4, 128.4, 106.3, 65.0, 56.7, 40.2, 25.8, 25.2, 20.6; MS (ESI) *m/z*: 354.2 $[M+H]^+$.

*4.1.5.2 (1-Carbamimidoylpiperidin-4-yl)methyl-4-acetoxy-3,5-dimethoxybenzoate (**12h**).*

Yield 83%, white solid, m.p. 158~162^{o}C. ^{1}H NMR (DMSO-d_6, 300 MHz): δ (ppm) 7.30 (s, 2H), 7.05-7.45 (br, 3H), 4.23 (m, 2H), 3.95 (m, 2H), 3.85 (s, 6H), 3.07 (t, J = 6.0, 2H), 2.30 (s, 3H), 2.12 (m, 1H), 1.87 (m, 2H), 1.30 (m, 2H); ^{13}C NMR (DMSO-d_6, 75 MHz): δ (ppm) 168.3, 165.2, 158.0, 152.5, 128.4, 106.5, 68.4, 56.2, 35.8, 20.3; MS (ESI) *m/z*: 380.2 $[M+H]^+$.

*4.1.6 Procedure for the Synthesis of Compounds **13a-13t**.*

The mixture of **6c** (1 equiv, 0.83 mmol)**,** various acids (1 equiv, 0.83 mmol), EDCI (1.2 equiv, 1.0 mmol), and DMAP (catalytic amount) were stirred in DCM (20 mL) at room temperature for 2-18 h. 20 mL DCM was added after the completion of the reaction, the organic layer was washed with water (20 mL) and brine (20 mL), dried over Na_2SO_4, and concentrated to afford crude products which were purified by flash chromatography (DCM/MeOH, 40:1) to provide **13a-13t** as white solids (83-98%).

*4.1.6.1 4-(2,3-Bis(tert-butoxycarbonyl)guanidino)butyl cyclohexanecarboxylate (**13a**).*

Yield 89%, white solid, m.p. 74~76^{o}C. ^{1}H NMR ($CDCl_3$, 300 MHz): δ (ppm) 11.44 (s, 1H), 8.27 (s, 1H), 4.01 (t, J = 6.0 Hz, 2H), 3.39 (t, J = 6.0 Hz, 2H), 2.23 (m, 1H), 1.82 (m, 2H), 1.67 (m, 7H), 1.46 (s, 9H), 1.45 (s, 9H), 1.42 (m, 2H), 1.34 (m, 3H); ^{13}C NMR ($CDCl_3$, 75 MHz): δ (ppm) 163.0, 155.6, 152.8, 140.1 82.5, 78.7, 63.0, 42.7, 39.9, 28.5, 27.8 27.5, 25.6, 25.2, 24.9; MS (ESI) *m/z*: 242.3 $[M-2Boc+H]^+$.

*4.1.6.2 2,3-Bis(tert-butoxycarbonyl)guanidino)butyl-adamantane-1-carboxylate (**13b**).*

Yield 85%, white solid, m.p. 110~112°C. ^{1}H NMR ($CDCl_3$, 300 MHz): δ (ppm) 11.45 (s, 1H), 8.27 (s, 1H), 4.00 (t, J = 5.2 Hz, 2H), 3.38 (d, J = 5.3 Hz, 2H), 1.94 (s, 3H), 1.81(s, 6H), 1.64(m, 10H), 1.44 (s, 9H), 1.43(s, 9H); ^{13}C NMR ($CDCl_3$, 75 MHz): δ (ppm) 177.0, 163.1, 155.6, 152.8, 82.5, 78.7, 63.0, 40.1, 39.9, 38.3, 36.0, 27.8, 27.5, 27.4, 25.6, 25.5; MS (ESI) *m/z*: 294.4 $[M\text{-}2Boc+H]^+$.

*4.1.6.3 4-(2,3-Bis(tert-butoxycarbonyl)guanidino)butyl furan-2-carboxylate (**13c**).* Yield 97%, white solid, m.p. 58~60°C. ^{1}H NMR ($CDCl_3$, 300 MHz): δ (ppm) 11.44 (s, 1H), 8.29 (s, 1H), 7.51 (s, 1H), 7.10 (d, J = 3.6 Hz, 1H), 6.43 (t, J = 1.8 Hz, 1H), 4.25 (t, J = 6.0 Hz, 2H), 3.41 (m, 2H), 1.71 (m, 2H), 1.67 (m, 2H), 1.42 (s, 9H), 1.41 (s, 9H); ^{13}C NMR ($CDCl_3$, 75 MHz): δ (ppm) 163.0, 158.1, 155.6, 152.7, 145.7, 144.1, 117.3, 111.2, 82.5, 78.6, 63.8, 39.8, 27.7, 27.5, 25.5, 25.2; MS (ESI) *m/z*: 326.2 $[M\text{-}Boc+H]^+$.

*4.1.6.4 4-(2,3-Bis(tert-butoxycarbonyl)guanidino)butyl isonicotinate (**13d**).* Yield 88%, white solid, m.p. 74~76°C. ^{1}H NMR ($CDCl_3$, 300 MHz): δ (ppm) 11.44 (s, 1H), 8.71 (d, J = 4.2 Hz, 2H), 8.30 (s, 1H), 7.77 (d, J = 4.2 Hz, 2H), 4.32 (t, J = 5.7 Hz, 2H), 3.43 (m, 2H), 1.78 (m, 2H), 1.68 (m, 2H), 1.43 (s, 9H), 1.42 (s, 9H); ^{13}C NMR ($CDCl_3$, 75 MHz): δ (ppm) 165.0, 163.5, 156.2, 153.3, 150.6, 137.4, 122.8, 83.1, 79.3, 65.2, 40.4, 28.3, 28.0, 26.0, 25.8; MS (ESI) *m/z*: 337.3 $[M\text{-}Boc+H]^+$.

*4.1.6.5 4-(2,3-Bis(tert-butoxycarbonyl)guanidino)butyl-1H-indole-5-carboxylate (**13e**).* Yield 83%, white solid, m.p. 131~132°C. ^{1}H NMR ($CDCl_3$, 300 MHz): δ (ppm) 11.43 (s, 1H), 8.79 (s, 1H), 8.32 (s, 2H), 7.80 (d, J = 8.1 Hz, 1H), 7.33 (d, J = 8.1 Hz, 1H), 7.20 (s, 1H), 6.57 (s, 1H), 4.24 (t, J = 6.0 Hz, 2H), 3.40 (t, J = 6.0 Hz, 2H), 1.68 (m, 4H), 1.42 (s, 9H), 1.41 (s, 9H); ^{13}C NMR ($CDCl_3$, 75 MHz): δ (ppm) 155.7, 152.8, 138.0, 127.0, 125.1, 123.2, 122.8, 121.4, 110.3, 103.4, 82.7, 78.9, 63.5, 40.1, 27.8, 27.6, 25.8, 25.4; MS (ESI) *m/z*: 375.2 $[M\text{-}Boc+H]^+$.

*4.1.6.6 4-(2,3-Bis(tert-butoxycarbonyl)guanidino)butyl-3-methylbenzoate (**13f**).* Yield 87%, white solid, m.p. 54~56°C. ^{1}H NMR ($CDCl_3$, 300 MHz): δ (ppm) 11.51 (s, 1H), 8.37 (s, 1H), 7.85 (m, 2H), 7.32 (m, 2H), 4.33 (t, J = 6.1 Hz, 2H), 3.49 (m, 2H), 2.40 (s, 3H), 1.78 (m, 4H), 1.50 (s, 9H), 1.49 (s, 9H); ^{13}C NMR ($CDCl_3$, 75 MHz): δ (ppm) 166.3, 156.2, 138.1, 133.7, 130.1, 128.2, 126.7, 83.1, 79.3, 64.3, 40.5, 28.2, 28.0, 26.2, 25.8, 21.3; MS (ESI) *m/z*: 250.3 $[M\text{-}2Boc+H]^+$.

*4.1.6.7 4-(2,3-Bis(tert-butoxycarbonyl)guanidino)butyl-2,4,6-trifluorobenzoate (**13g**).* Yield 95%, white solid, m.p. 72~74°C. ^{1}H NMR ($CDCl_3$, 300 MHz): δ (ppm) 11.51 (s, 1H), 8.36 (s, 1H), 7.35 (s, 2H), 4.42 (t, J = 6.1 Hz, 2H), 3.49 (m, 2H), 1.75 (m, 4H), 1.50 (s, 9H), 1.49 (s, 9H); ^{13}C NMR ($CDCl_3$, 75 MHz): δ (ppm) 163.9, 163.5, 156.2, 153.3, 136.1, 132.5, 132.2, 127.9, 83.1, 79.2, 65.9, 40.2, 28.2, 28.0, 25.9, 25.6; MS (ESI) *m/z*: 390.4 $[M\text{-}Boc+H]^+$.

*4.1.6.8 4-(2,3-Bis(tert-butoxycarbonyl)guanidino)butyl 4-nitrobenzoate (**13h**).* Yield 95%, white solid, m.p. 88~90°C. ^{1}H NMR ($CDCl_3$, 300 MHz): δ (ppm) 11.43 (s, 1H), 8.33 (s, 1H), 8.22, 8.13 (dd, $J_A = J_B$ = 8.9 Hz, each 2H), 4.33 (t, J = 6.2 Hz, 2H), 3.45 (m, 2H), 1.78 (m, 2H), 1.69 (m, 2H), 1.42 (s, 9H), 1.41 (s, 9H); ^{13}C NMR ($CDCl_3$, 75 MHz): δ (ppm) 164.1, 155.6, 152.8, 135.1, 130.2, 123.0, 82.8, 79.0, 64.9, 40.0, 27.8, 27.5, 25.5, 25.3; MS (ESI) *m/z*: 281.2 $[M\text{-}2Boc+H]^+$.

*4.1.6.9 4-(2,3-Bis(tert-butoxycarbonyl)guanidino)butyl-4-(trifluoromethyl)benzoate (**13i**).* Yield 96%, white solid, m.p. 132~133°C. ^{1}H NMR ($CDCl_3$, 300 MHz): δ (ppm) 11.45 (s, 1H), 8.40 (s, 1H), 8.08, 7.63 (dd, $J_A = J_B$ = 8.1 Hz, each 2H), 4.32 (t, J = 6.1 Hz, 2H), 3.49 (m, 2H), 1.74 (m, 4H), 1.42 (s, 9H), 1.41 (s, 9H); ^{13}C NMR ($CDCl_3$, 75 MHz): δ (ppm) 166.3, 163.0, 155.6, 152.9, 152.8, 144.2, 129.4, 116.7, 104.6, 82.6, 78.7, 63.4, 60.4, 55.6, 39.9, 27.7, 27.5, 25.6, 25.3; MS (ESI) *m/z*: 404.2 $[M\text{-}Boc+H]^+$.

*4.1.6.10 4-(2,3-Bis(tert-butoxycarbonyl)guanidino)butyl-4-acetoxybenzoate (**13j**).* Yield 84%, white solid, m.p. 76~80°C. ^{1}H NMR ($CDCl_3$, 300 MHz): δ (ppm) 11.54 (s, 1H), 8.39 (s, 1H), 8.08 (d, J = 3.0 Hz, 2H), 7.16 (d, J = 3.0 Hz, 2H), 4.32 (t, J = 6.0 Hz, 2H), 3.49 (m, 2H), 2.35 (s, 3H), 1.74 (m, 4H), 1.42 (s, 9H), 1.41 (s, 9H); ^{13}C NMR ($CDCl_3$, 75 MHz): δ (ppm) 168.7, 165.6, 163.5, 156.1, 154.2, 153.2, 131.1, 127.7, 121.5, 83.0, 79.1, 64.5, 40.3, 28.2, 27.9, 26.1, 25.7, 21.1; MS (ESI) *m/z*: 394.2 $[M\text{-}Boc+H]^+$.

*4.1.6.11 4-(2,3-Bis(tert-butoxycarbonyl)guanidino)butyl 2-acetoxybenzoate (**13k**).* Yield 89%, white solid, m.p. 57~60°C. ^{1}H NMR ($CDCl_3$, 300 MHz): δ (ppm) 11.51 (s, 1H), 8.37 (s, 1H), 8.01 (d, J = 3.0 Hz, 1H), 7.55 (t, J = 5.1 Hz, 1H), 7.31 (t, J = 5.1 Hz, 1H), 7.11 (d, J = 3.0 Hz, 1H), 4.29 (t, J = 6.1 Hz, 2H), 3.49 (m, 2H), 2.35 (s, 3H), 1.78 (m, 4H), 1.50 (s, 9H), 1.49 (s, 9H); ^{13}C NMR ($CDCl_3$, 75 MHz): δ (ppm) 164.4, 163.4,

156.2, 153.5, 150.5, 133.9, 131.6, 126.4, 123.7, 82.9, 79.5, 64.6, 40.5, 28.5, 28.1, 26.3, 25.7, 20.9; MS (ESI) *m/z*: 394.2 $[M\text{-}Boc+H]^+$.

*4.1.6.12 4-(2,3-Bis(tert-butoxycarbonyl)guanidino)butyl 3-acetoxybenzoate (**13l**).* Yield 92%, white solid, m.p. 80~82°C. ^{1}H NMR ($CDCl_3$, 300 MHz): δ (ppm) 11.52 (s, 1H), 8.38 (s, 1H), 7.92 (d, J = 3.0 Hz, 1H), 7.74 (s, 1H), 7.46 (t, J = 3.0 Hz, 1H), 7.29 (d, J = 3.0 Hz, 1H), 4.34 (t, J = 6.0 Hz, 2H), 3.49 (m, 2H), 2.33 (s, 3H), 1.78 (m, 4H), 1.50 (s, 9H), 1.49 (s, 9H); ^{13}C NMR ($CDCl_3$, 75 MHz): δ (ppm) 169.2, 165.6, 163.6, 156.2, 153.3, 150.6, 131.8, 129.4, 127.0, 126.3, 122.8, 83.1, 79.3, 64.7, 40.4, 28.3, 28.0, 26.1, 26.8, 21.1; MS (ESI) *m/z*: 394.2 $[M\text{-}Boc+H]^+$.

4.1.6.13

*4-(2,3-Bis(tert-butoxycarbonyl)guanidino)butyl-4-acetoxy-3-methoxybenzoate (**13m**).* Yield 92%, white solid, m.p. 102~105°C. ^{1}H NMR ($CDCl_3$, 300 MHz): δ (ppm) 11.55 (s, 1H), 8.39 (s, 1H), 7.68 (d, J = 4.5 Hz, 1H), 7.65 (s, 1H), 7.1 (d, J = 4.5 Hz, 1H), 4.35 (t, J = 6.0 Hz, 2H), 3.88 (s, 3H) 3.49 (m, 2H), 2.31(s, 3H), 1.74 (m, 4H), 1.42 (s, 9H), 1.41 (s, 9H); ^{13}C NMR ($CDCl_3$, 75 MHz): δ (ppm) 168.2, 165.5, 163.4, 156.1, 153.1, 150.1, 143.5, 128.8, 122.7, 122.4, 113.2, 82.9, 79.0, 64.5, 55.9, 40.3, 28.1, 27.9, 26.0, 25.7, 20.4; MS (ESI) *m/z*: 524.3 $[M+H]^+$.

*4.1.6.14 4-(2,3-Bis(tert-butoxycarbonyl)guanidino)butyl 4-methoxybenzoate (**13n**).* Yield 94%, white solid, m.p. 95~96°C. ^{1}H NMR ($CDCl_3$, 300 MHz): δ (ppm) 11.44 (s, 1H), 8.29 (s, 1H), 7.92 (d, J = 4.2 Hz, 2H), 6.85 (d, J = 4.2 Hz, 2H), 4.24 (t, J = 6.0 Hz, 2H), 3.77 (s, 3H), 3.42 (m, 2H), 1.72 (m, 4H), 1.43 (s, 9H), 1.42 (s, 9H); ^{13}C NMR ($CDCl_3$, 75 MHz): δ (ppm) 166.2, 163.6, 163.3, 156.2, 153.3, 131.7, 122.7, 113.6, 83.1, 79.2, 64.1, 55.4, 40.5, 28.3, 28.1, 26.2, 25.9; MS (ESI) *m/z*: 266.3 $[M\text{-}2Boc+H]^+$.

*4.1.6.15 4-(2,3-Bis(tert-butoxycarbonyl)guanidino)butyl 2,3-dimethoxybenzoate (**13o**).* Yield 93%, white solid, m.p. 66~70°C. ^{1}H NMR ($CDCl_3$, 300 MHz): δ (ppm) 11.51 (s, 1H), 8.39 (s, 1H), 7.31 (s, 1H), 7.07 (s, 2H), 4.34 (s, 2H), 3.89 (s, 6H), 3.49 (s, 2H), 1.79 (s, 4H), 1.49 (s, 9H), 1.48 (s, 9H); ^{13}C NMR ($CDCl_3$, 75 MHz): δ (ppm) 166.2, 163.5, 156.1, 153.4, 153.2, 126.2, 123.8, 122.1, 115.7, 83.0, 79.2, 64.5, 61.4, 55.9, 40.4, 28.2, 27.9, 26.1, 25.7; MS (ESI) *m/z*: 296.3 $[M\text{-}2Boc+H]^+$.

*4.1.6.16 4-(2,3-Bis(tert-butoxycarbonyl)guanidino)butyl 2,5-dimethoxybenzoate (**13p**).*

Yield 91%, white solid, m.p. 76~77°C. ^{1}H NMR ($CDCl_3$, 300 MHz): δ (ppm) 11.51 (s, 1H), 8.37 (s, 1H), 7.31 (s, 1H), 7.03 (d, *J* = 4.2 Hz, 1H), 6.92 (d, *J* = 4.2 Hz, 1H), 4.33 (m, 2H), 3.85 (s, 3H), 3.79 (s, 3H), 3.49 (m, 2H), 1.79 (m, 4H), 1.49 (s, 9H), 1.48 (s, 9H); ^{13}C NMR ($CDCl_3$, 75 MHz): δ (ppm) 166.2, 163.6, 156.2, 153.4, 153.3, 119.3, 116.0, 113.8, 83.1, 79.2, 64.4, 56.6, 55.8, 40.5, 28.2, 28.0, 26.1, 25.8; MS (ESI) *m/z*: 296.3 $[M\text{-}2Boc+H]^+$.

4.1.6.17 4-(2,3-Bis(tert-butoxycarbonyl)guanidino)butyl-2,3,4-trimethoxybenzoate ***(13q)****.* Yield 89%, white solid, m.p. 51~56°C. ^{1}H NMR ($CDCl_3$, 300 MHz): δ (ppm) 11.52 (s, 1H), 8.39 (s, 1H), 7.60 (d, *J* = 4.2 Hz, 1H), 6.71 (d, *J* = 4.2 Hz, 1H), 4.32 (t, *J* = 6.0 Hz, 2H), 3.92 (s, 3H), 3.88 (s, 3H), 3.87 (s, 3H), 3.49 (m, 2H), 1.74 (m, 4H), 1.42 (s, 9H), 1.41 (s, 9H); ^{13}C NMR ($CDCl_3$, 75 MHz): δ (ppm) 165.5, 163.5, 161.3, 157.1, 156.1, 154.6, 153.2, 142.9, 126.9, 117.9, 106.9, 83.1, 79.2, 64.2, 61.7, 60.9, 56.0, 40.5, 28.3, 28.0, 26.1, 25.8; MS (ESI) *m/z*: 326.3 $[M\text{-}2Boc+H]^+$.

4.1.6.18 4-(2,3-Bis(tert-butoxycarbonyl)guanidino)butyl-2,4,6-trimethoxybenzoate ***(13r)****.*

Yield 86%, white solid, m.p. 62~65°C. ^{1}H NMR ($CDCl_3$, 300 MHz): δ (ppm) 11.50 (s, 1H), 8.35 (s, 1H), 6.84 (s, 2H), 4.33 (t, *J* = 6.1 Hz, 2H), 3.53 (m, 2H), 2.27 (s, 9H), 1.79 (m, 4H), 1.50 (s, 9H), 1.49 (s, 9H); ^{13}C NMR ($CDCl_3$, 75 MHz): δ (ppm) 156.2, 153.5, 135.0, 128.4, 83.1, 79.3, 64.3, 40.4, 28.3, 28.0, 26.2, 25.8, 21.1, 19.8; MS (ESI) *m/z*: 326.4 $[M\text{-}2Boc+H]^+$.

4.1.6.19 4-(2,3-Bis(tert-butoxycarbonyl)guanidino)butyl 3,4,5-trimethoxybenzoate ***(13s)****.*

Yield 89%, white solid, m.p. 85~86°C. ^{1}H NMR ($CDCl_3$, 300 MHz): δ (ppm) 11.52 (s, 1H), 8.39 (s, 1H), 7.32 (d, *J* = 4.2 Hz, 2H), 4.36 (m, 2H), 3.92 (s, 9H), 3.53 (m, 2H), 1.82 (m, 4H), 1.53 (s, 9H), 1.52 (s, 9H); ^{13}C NMR ($CDCl_3$, 75 MHz): δ (ppm) 166.0, 163.5, 156.1, 153.2, 152.8, 125.2, 106.7, 83.0, 79.1, 64.5, 60.7, 56.1, 40.3, 28.2, 27.9, 26.1, 25.8; MS (ESI) *m/z*: 326.3 $[M\text{-}2Boc+H]^+$.

4.1.6.20

4-((E)-2,3-bis(tert-butoxycarbonyl)guanidino)butyl-3-(3,4,5-trimethoxyphenyl) acrylate ***(13t)****.*

Yield 92%, white solid, m.p. 93~94°C. ^{1}H NMR ($CDCl_3$, 300 MHz): δ (ppm) 11.45 (s, 1H), 8.32 (s, 1H), 7.52, 6.27 (dd, $J_A = J_B$=15.9 Hz, each 1H), 6.69 (s, 2H), 4.16 (t, J = 5.5 Hz, 2H), 3.81 (t, J = 2.1 Hz, 9H), 3.43 (d, J = 5.1 Hz, 2H), 1.68 (s, 4H), 1.43 (s, 9H), 1.42 (s, 9H); ^{13}C NMR ($CDCl_3$, 75 MHz): δ (ppm) 166.4, 155.6, 152.9, 152.8, 144.3, 129.4, 116.8, 104.7, 82.7, 63.5, 60.4, 55.6, 40.1, 27.8, 27.5, 25.7, 25.3; MS (ESI) *m/z*: 352.3 $[M-2Boc+H]^+$.

*4.1.7 Procedure for the Synthesis of Compounds **14a-14t**.*

Compounds **13a-13t** (1 equiv, 0.41 mmol) and zinc bromide (5 equiv, 2.1 mmol) were stirred in DCM at r.t. for 1-24h. Then, the crude products were purified by flash chromatography using DCM/MeOH 10:1 (v/v) as eluent, furnish **14a-14t** as white solids (83-98%).

*4.1.7.1 4-Guanidinobutyl-cyclohexanecarboxylate (**14a**).*

Yield 83%, white solid, m.p. 120~121°C. ^{1}H NMR (DMSO-d_6, 300 MHz): δ (ppm) 7.42 (m, 1H), 6.25-7.25 (br, 3H), 4.11 (t, J = 6.0 Hz, 2H), 3.18 (t, J = 6.0 Hz, 2H), 2.21 (m, 1H), 1.89 (m, 2H), 1.65 (m, 7H), 1.41 (m, 2H), 1.37 (m, 3H); ^{13}C NMR (DMSO-d_6, 75 MHz): δ (ppm) 172.1, 156.1, 64.2, 41.7, 39.5, 27.2, 25.2, 25.5, 25.1; MS (ESI) *m/z*: 242.1 $[M+H]^+$.

*4.1.7.2 4-Guanidinobutyl-adamantane-1-carboxylate (**14b**).*

Yield 78%, white solid, m.p. 137~139°C. ^{1}H NMR (DMSO-d_6, 300 MHz): δ (ppm) 7.47(m, 1H), 6.75-7.25 (br, 3H), 4.00 (t, J = 5.2 Hz, 2H), 3.15 (m, 2H), 1.95 (s, 3H), 1.80 (s, 6H), 1.65 (m, 10H); ^{13}C NMR (DMSO-d_6, 75 MHz): δ (ppm) 176.9, 153.6, 63.5, 41.1, 38.9, 36.4, 25.7, 25.0; MS (ESI) *m/z*: 294.1 $[M+H]^+$.

*4.1.7.3 4-Guanidinobutyl-furan-2-carboxylate (**14c**).*

Yield 94%, white solid, m.p. 107~108°C. ^{1}H NMR (DMSO-d_6, 300 MHz): δ (ppm) 7.98 (d, J = 3.6 Hz, 1H), 7.50 (m, 1H), 7.31 (t, J = 3.6 Hz, 1H), 6.71 (t, J = 1.8 Hz, 1H), 6.75-7.45 (br, 3H), 4.26 (m, 2H), 3.14 (m, 2H), 1.70 (m, 2H), 1.58 (m, 2H); ^{13}C NMR (DMSO-d_6, 75 MHz): δ (ppm) 157.8, 156.7, 147.5, 143.7, 118.3, 112.2, 63.9, 40.2, 25.2, 25.1; MS (ESI) *m/z*: 226.1 $[M+H]^+$.

*4.1.7.4 4-Guanidinobutyl isonicotinate (**14d**).*

Yield 92%, white solid, m.p. 116~119°C. ^{1}H NMR (DMSO-d_6, 300 MHz): δ (ppm) 8.73

(d, J = 4.2 Hz, 2H), 7.97 (d, J = 4.2 Hz, 2H), 7.46 (m, 1H), 6.70-7.20 (br, 3H), 4.28 (m, 2H), 3.23 (m, 2H), 1.72 (m, 2H), 1.65 (m, 2H); ^{13}C NMR (DMSO-d_6, 75 MHz): δ (ppm) 165.0, 157.2, 150.0, 137.3, 122.4, 63.7, 39.5, 27.3, 25.2; MS (ESI) *m/z*: 237.2 $[M+H]^+$.

*4.1.7.5 4-Guanidinobutyl-1H-indole-5-carboxylate (**14e**).*

Yield 81%, white solid, m.p. 176~181^{o}C. ^{1}H NMR (DMSO-d_6, 300 MHz): δ (ppm) 8.27 (s, 1H), 7.80 (d, J = 8.1 Hz, 1H), 7.43 (m, 1H), 7.32 (d, J = 8.1 Hz, 1H), 7.28 (s, 1H), 6.75-7.25 (br, 3H), 6.63 (s, 1H), 4.21 (t, J = 6.0 Hz, 2H), 3.18 (m, 2H), 1.71 (m, 2H), 1.62 (m, 2H); ^{13}C NMR (DMSO-d_6, 75 MHz): δ (ppm) 165.9, 158.1, 138.2, 128.1, 125.2, 123.0, 121.9, 110.1, 103.64, 64.1, 40.2, 25.9, 25.3; MS (ESI) *m/z*: 275.2 $[M+H]^+$.

*4.1.7.6 4-Guanidinobutyl-3-methylbenzoate (**14f**).*

Yield 93%, white solid, m.p. 108~111^{o}C. ^{1}H NMR (DMSO-d_6, 300 MHz): δ (ppm) 7.75 (m, 2H), 7.46 (m, 2H), 7.42 (m, 1H), 6.75-7.25 (br, 3H), 4.26 (t, J = 6.1 Hz, 2H), 3.16 (m, 2H), 2.36 (s, 3H), 1.72 (m, 2H), 1.61 (m, 2H); ^{13}C NMR (DMSO-d_6, 75 MHz): δ (ppm) 166.3, 157.1, 138.6, 134.4, 130.2, 129.9, 129.2, 126.7, 64.6, 40.8, 25.9, 25.6, 21.3; MS (ESI) *m/z*: 250.1 $[M+H]^+$.

*4.1.7.7 4-Guanidinobutyl-2,4,6-trifluorobenzoate (**14g**).*

Yield 90%, white solid, m.p. 116~117^{o}C. ^{1}H NMR (DMSO-d_6, 300 MHz): δ (ppm) 7.44 (m, 1H), 7.31 (s, 2H), 6.75-7.25 (br, 3H), 4.38 (t, J = 6.1 Hz, 2H), 3.19 (m, 2H), 1.72 (m, 2H), 1.61 (m, 2H); ^{13}C NMR (DMSO-d_6, 75 MHz): δ (ppm) 165.1, 163.5, 155.3, 152.7, 135.2, 126.9, 65.2, 40.4, 25.2, 25.1; MS (ESI) *m/z*: 290.1 $[M+H]^+$.

*4.1.7.8 4-Guanidinobutyl-4-nitrobenzoate (**14h**).*

Yield 87%, white solid, m.p. 118~119^{o}C. ^{1}H NMR (DMSO-d_6, 300 MHz): δ (ppm) 8.13, 7.70 (dd, J_A = J_B = 8.9 Hz, each 2H), 7.42 (m, 1H), 6.75-7.25 (br, 3H), 4.39 (t, J = 6.2 Hz, 2H), 4.07 (m, 2H), 1.72 (m, 2H), 1.59 (m, 2H); ^{13}C NMR (DMSO-d_6, 75 MHz): δ (ppm) 164.7, 157.0, 150.6, 135.6, 131.0, 124.3, 65.5, 49.1, 25.7, 25.5; MS (ESI) *m/z*: 481.2 $[M+H]^+$.

*4.1.7.9 4-Guanidinobutyl-4-(trifluoromethyl)benzoate (**14i**).*

Yield 83%, white solid, m.p. >200^{o}C. ^{1}H NMR (DMSO-d_6, 300 MHz): δ (ppm) 7.45 (m, 1H), 7.63, 6.69 (dd, J_A = J_B = 8.1 Hz, each 2H), 6.75-7.25 (br, 3H), 4.18 (t, J = 6.1 Hz, 2H), 3.24 (m, 2H), 1.67 (m, 4H); ^{13}C NMR (DMSO-d_6, 75 MHz): δ (ppm) 166.8, 153.6,

139.9, 117.7, 63.9, 41.2, 25.8, 25.1; MS (ESI) *m/z*: 304.1 $[M+H]^+$.

*4.1.7.10 4-Guanidinobutyl-4-acetoxybenzoate (**14j**).*

Yield 93%, white solid, m.p. 112~113°C. ^{1}H NMR (DMSO-d_6, 300 MHz): δ (ppm) 8.01 (d, J = 8.7 Hz, 1H), 7.31 (d, J = 8.7 Hz, 1H), 7.46 (m, 1H), 6.75-7.25 (br, 3H), 4.30 (t, J = 6.0 Hz, 2H), 3.17 (m, 2H), 2.30 (s, 3H), 1.73 (m, 2H), 1.62 (m, 2H); ^{13}C NMR (DMSO-d_6, 75 MHz): δ (ppm) 169.3, 165.5, 157.0, 154.7, 131.2, 127.7, 122.8, 122.8, 64.7, 40.3, 25.9, 25.6, 21.4; MS (ESI) *m/z*: 294.2 $[M+H]^+$.

*4.1.7.11 4-Guanidinobutyl-2-acetoxybenzoate (**14k**).*

Yield 90%, white solid, m.p. 107~108°C. ^{1}H NMR (DMSO-d_6, 300 MHz): δ (ppm) 8.04 (d, J = 3.0 Hz, 1H), 7.56 (t, J = 5.1 Hz, 1H), 7.44 (m, 1H), 7.35 (t, J = 5.1 Hz, 1H), 7.10 (d, J = 3.0 Hz, 1H), 6.75-7.25 (br, 3H), 4.32 (t, J = 6.0 Hz, 2H), 3.15 (m, 2H), 2.31 (s, 3H), 1.72 (m, 2H), 1.62 (m, 2H); ^{13}C NMR (DMSO-d_6, 75 MHz): δ (ppm) 170.3, 161.3, 153.3, 151.8, 133.1, 130.3, 117.6, 116.2, 63.3, 40.2, 25.2, 24.5, 20.7; MS (ESI) *m/z*: 294.2 $[M+H]^+$.

*4.1.7.12 4-Guanidinobutyl-3-acetoxybenzoate (**14l**).*

Yield 86%, white solid, m.p. 124~125°C. ^{1}H NMR (DMSO-d_6, 300 MHz): δ (ppm) 7.91 (d, J = 3.0 Hz, 1H), 7.71 (m, 1H), 7.42 (t, J = 3.0 Hz, 1H), 7.44 (m, 1H), 7.28 (d, J = 3.0 Hz, 1H), 6.75-7.25 (br, 3H), 4.31 (t, J = 6.0 Hz, 2H), 3.13 (m, 2H), 2.30 (s, 3H), 1.74 (m, 4H); ^{13}C NMR (DMSO-d_6, 75 MHz): δ (ppm) 167.8, 164.0, 156.5, 149.3, 129.8, 127.7, 124.8, 120.8, 62.7, 39.3, 23.9, 23.0, 19.9; MS (ESI) *m/z*: 294.2 $[M+H]^+$.

*4.1.7.13 4-Guanidinobutyl-4-acetoxy-3-methoxybenzoate (**14m**).*

Yield 87%, white solid, m.p. 128~129°C. ^{1}H NMR (DMSO-d_6, 300 MHz): δ (ppm) 7.59 (d, J = 4.5 Hz, 1H), 7.55 (s, 1H), 7.42 (m, 1H), 7.15 (d, J = 4.5 Hz, 1H), 6.75-7.25 (br, 1H), 4.31 (t, J = 6.0 Hz, 2H), 3.79 (s, 3H), 3.19 (m, 2H), 2.18 (s, 3H), 1.69 (m, 2H), 1.62 (m, 2H); ^{13}C NMR (DMSO-d_6, 75 MHz): δ (ppm) 169.2, 165.8, 158.1, 143.6, 128.9, 123.7, 122.6, 113.3, 64.9, 56.4, 41.2, 25.6, 24.8, 20.7; MS (ESI) *m/z*: 324.1 $[M+H]^+$.

*4.1.7.14 4-Guanidinobutyl-4-methoxybenzoate (**14n**).*

Yield 92%, white solid, m.p. 131~132°C. ^{1}H NMR (DMSO-d_6, 300 MHz): δ (ppm) 7.92, 7.08 (d, J = 8.7 Hz, each 1H), 7.47 (m, 1H), 6.75-7.25 (br, 3H), 4.42 (t, J = 5.5 Hz,

2H), 3.81 (s, 3H), 3.16 (m, 2H), 1.72 (m, 2H), 1.63 (m, 2H); ^{13}C NMR (DMSO-d_6, 75 MHz): δ (ppm) 167.5, 163.3, 158.0, 131.8, 123.4, 114.2, 63.8, 55.9, 40.0, 25.3, 25.2; MS (ESI) *m/z*: 266.2 $[M+H]^+$.

*4.1.7.14 4-Guanidinobutyl-2,3-dimethoxybenzoate (**14o**).*

Yield 81%, white solid, m.p. 109~110^{o}C. ^{1}H NMR (DMSO-d_6, 300 MHz): δ (ppm) 7.46 (m, 1H), 7.15 (m, 1H), 7.10 (m, 2H), 6.75-7.45 (br, 3H), 4.26 (t, J = 6.0 Hz, 2H), 3.72 (s, 3H), 3.66 (s, 3H), 3.22 (m, 2H), 1.63 (m, 4H); ^{13}C NMR (DMSO-d_6, 75 MHz): δ (ppm) 166.5, 158.1, 156.2, 147.3, 125.3, 124.4, 121.1, 116.2, 64.5, 60.9, 55.7, 40.6, 24.9, 24.0; MS (ESI) *m/z*: 296.2 $[M+H]^+$; HR-MS (ESI) *m/z*: calcd for $C_{14}H_{22}N_3O_4$ $[M + H]^+$, 296.1605; found 296.1631.

*4.1.7.16 4-Guanidinobutyl-2,5-dimethoxybenzoate (**14p**).*

Yield 83%, white solid, m.p. 124~126^{o}C. ^{1}H NMR (DMSO-d_6, 300 MHz): δ (ppm) 7.45 (m, 1H), 7.15 (d, J = 4.2 Hz, 1H), 7.11 (d, J = 4.2 Hz, 1H), 6.75-7.25 (br, 3H), 4.23 (m, 2H), 3.76 (s, 3H), 3.72 (s, 3H), 3.13 (m, 2H), 1.69 (m, 2H), 1.64 (m, 2H); ^{13}C NMR (DMSO-d_6, 75 MHz): δ (ppm) 166.0, 153.0, 152.7, 121.5, 119.0, 115.8, 114.7, 64.5, 56.9, 56.1, 40.3, 25.7, 25.1; MS (ESI) *m/z*: 296.2 $[M+H]^+$.

*4.1.7.17 4-Guanidinobutyl-2,3,4-trimethoxybenzoate (**14q**).*

Yield 85%, white solid, m.p. 119~121^{o}C. ^{1}H NMR (DMSO-d_6, 300 MHz): δ (ppm) 7.48 (d, J = 4.2 Hz, 1H), 7.46 (m, 1H), 6.92 (d, J = 4.2 Hz, 1H), 6.75-7.45 (br, 3H), 4.26 (t, J = 6.0 Hz, 2H), 3.86 (s, 3H), 3.79 (s, 3H), 3.75 (s, 3H), 3.18 (m, 2H), 1.72 (m, 4H); ^{13}C NMR (DMSO-d_6, 75 MHz): δ (ppm) 165.8, 160.3, 158.1, 156.2, 143.1, 127.1, 117.8, 106.9, 64.5, 61.6, 60.4, 56.1, 41.5, 26.1, 25.9; MS (ESI) *m/z*: 326.2 $[M+H]^+$.

*4.1.7.18 4-Guanidinobutyl-2,4,6-trimethoxybenzoate (**14r**).*

Yield 86%, white solid, m.p. 118~120^{o}C.^{1}H NMR (DMSO-d_6, 300 MHz): δ (ppm) 7.46 (m, 2H), 6.90 (m, 2H), 6.75-7.25 (br, 3H), 4.21 (t, J = 6.1 Hz, 2H), 3.30 (m, 2H), 2.24 (s, 3H), 2.20 (s, 6H), 1.72 (m, 2H), 1.59 (m, 2H); ^{13}C NMR (DMSO-d_6, 75 MHz): δ (ppm) 169.6, 156.2, 139.2, 134.7, 131.5, 128.6, 64.6, 55.2, 40.8, 25.7, 25.2; MS (ESI) *m/z*: 326.2 $[M+H]^+$.

*4.1.7.19 4-Guanidinobutyl-3,4,5-trimethoxybenzoate (**14s**).*

Yield 79%, white solid, m.p. 122~124^{o}C. ^{1}H NMR (DMSO-d_6, 300 MHz): δ (ppm)

7.42 (m, 1H), 7.19 (s, 2H), 6.75-7.20 (br, 3H), 4.25 (m, 2H), 3.80 (s, 6H), 3.62 (s, 3H), 3.14 (m, 2H), 1.73 (m, 2H), 1.55 (m, 2H); ^{13}C NMR (DMSO-d_6, 75 MHz): δ (ppm) 165.8, 157.0, 153.2, 142.5, 125.3, 106.8, 64.8, 60.7, 56.5, 40.8, 25.8, 25.6; MS (ESI) *m/z*: 326.2 $[M+H]^+$.

*4.1.7.20 4-Guanidinobutyl-3-(3,4,5-trimethoxyphenyl)acrylate (**14t**).*

Yield 83%, white solid, m.p. 128~130^{o}C. ^{1}H NMR (DMSO-d_6, 300 MHz): δ (ppm) 7.52, 6.27 (dd, $J_A = J_B$=15.9 Hz, each 1H), 7.48 (m, 1H), 6.75-7.25 (br, 3H), 6.73 (s, 2H), 4.43 (t, J = 5.5 Hz, 2H), 3.48 (s, 9H), 3.46 (t, J = 5.1 Hz, 2H), 1.78 (s, 4H); ^{13}C NMR (DMSO-d_6, 75 MHz): δ (ppm) 166.5, 157.0, 153.0, 145.2, 129.1, 116.5, 104.2, 63.8, 60.1, 56.1, 40.0, 25.6, 25.1; MS (ESI) *m/z*: 351.2 $[M+H]^+$.

*4.1.8 Procedure for the Synthesis of Compounds **17a-17c**.*

The mixture of **8** (1 equiv, 0.83 mmol), amino alcohols (1 equiv, 0.83 mmol), EDCI (1.2 equiv, 1.0 mmol), and DMAP (catalytic amount) were stirred in DCM (20 mL) at room temperature for 12 h. 20 mL DCM was added after the completion of the reaction, the organic layer was washed with water (20 mL) and brine (20 mL), dried over Na_2SO_4, and concentrated to afford **16a-d** without purification. To the solution of **16a-d** in anhydrous methanol, NaOH (1 equiv) was added and stirred at room temperature for 5-8 min. Concentration to dryness afforded crude products which were purified by flash chromatography (DCM/MeOH, 40:1) to provide **17a-d** as white solids (73-91%).

*4.1.8.1 2-(Dimethylamino)-ethyl-4-hydroxy-3,5-dimethoxybenzoate (**17a**).*

Yield 73%, white solid, m.p. 118~120^{o}C. ^{1}H NMR ($CDCl_3$, 300 MHz): δ (ppm) 7.09 (s, 2H), 4.44 (t, J = 6.0 Hz, 2H), 3.84 (s, 6H), 2.76 (t, J = 6.0 Hz, 2H), 2.38 (s, 6H); ^{13}C NMR ($CDCl_3$, 75 MHz): δ (ppm) 166.5, 146.9, 140.3, 119.6, 106.3, 61.6, 57.8, 56.0, 45.4; MS (ESI) *m/z*: 270.1 $[M+H]^+$.

*4.1.8.2 3-(Dimethylamino)-propyl-4-hydroxy-3,5-dimethoxybenzoate (**17b**).*

Yield 91%, white solid, m.p. 122~124^{o}C. ^{1}H NMR ($CDCl_3$, 300 MHz): δ (ppm) 7.30 (s, 2H), 4.35 (t, J = 6.0 Hz, 2H), 3.91 (s, 6H), 2.46 (t, J = 6.0 Hz, 2H), 2.23 (s, 6H), 1.97 (m, 2H); ^{13}C NMR ($CDCl_3$, 75 MHz): δ (ppm) 146.8, 139.7, 106.6, 63.2, 56.4, 56.2, 45.3, 26.9; MS (ESI) *m/z*: 284.1 $[M+H]^+$.

*4.1.8.3 2-(Diethylamino)-ethyl-4-hydroxy-3,5-dimethoxybenzoate (**17c**).*

Yield 77%, white solid, m.p. 59~61°C. ^{1}H NMR ($CDCl_3$, 300 MHz): δ (ppm) 7.25 (s, 2H), 6.25 (br, 1H), 4.31 (t, J = 6.0 Hz, 2H), 3.82 (s, 6H), 2.81 (t, J = 6.0 Hz, 2H), 2.61 (q, J = 6.9 Hz, 4H), 1.02 (t, J = 6.9 Hz, 6H); ^{13}C NMR ($CDCl_3$, 75 MHz): δ (ppm) 166.4, 146.8, 139.6, 120.7, 106.6, 63.0, 56.2, 50.9, 47.6, 11.6; MS (ESI) *m/z*: 298.1 $[M+H]^+$.

*4.1.8.4 2-Morpholinoethyl-4-hydroxy-3,5-dimethoxybenzoate (**17d**).*

Yield 85%, white solid, m.p. >200°C. ^{1}H NMR (DMSO-d_6, 300 MHz): δ (ppm) 9.41 (br, 1H), 7.31 (s, 2H), 4.61 (s, 2H), 3.93 (s, 4H), 3.83 (s, 6H), 3.53 (s, 4H), 3.21 (s, 2H); ^{13}C NMR (DMSO-d_6, 75 MHz): δ (ppm) 174.5, 147.5, 140.9, 118.6, 107.2, 63.0, 58.6, 56.2, 54.4, 51.2; MS (ESI) *m/z*: 312.1 $[M+H]^+$.

4.2 Cell Culture and Treatment.

H9c2 cells were purchased from ATCC. The cells were cultured in high glucose Dulbecco's modified Eagle's medium (DMEM) supplemented with 10% fetal bovine serum at 37 °C in an incubator with 5% CO_2. Cells at 80-90% confluence were used for experiments. Before treatment, H9c2 were exposed to serum starvation for 12 hours followed by treatment with compounds for 4 hours. Then the culture medium was substituted with DMEM containing 500 nM H_2O_2 and cells were incubated for another 1 hour before collected for biochemical assay.

4.3 Cell Viability Assay.

Briefly, H9c2 cells were released from plate by trypsin, centrifuged and re-suspended in DMEM medium at 1×10^5 cell/mL. 100 μL of the dilutions were plated out into wells of a 96-well microtiter plate in triplicate. Three control wells with medium alone was used to provide the blank absorbance. Cells were incubated for 18 hours before treated with tested compounds. SCM-198 analogs were diluted with DMSO to 1 and 10 μM. Cells were pre-treated with different concentrations of compounds for another 4 hours followed by stimulation with 400 nM hydrogen peroxide (H_2O_2) for 1 hour. Cells treated with SCM-198 were used as positive control and cells treated with DMSO alone were used as negative control. After stimulation, culture medium was carefully removed and 100 μL of MTT reagent was added to each well, and plates

were returned to cell culture incubator for 2 to 4 hours. When the purple precipitate is clearly visible under the microscope, the MTT regent was removed and 100 μL of DMSO was added to all wells to solve formazan. The absorbance in each well was measured at 570 nm in a microtiter plate reader.

4.4 LDH Release Detection.

Cells were seeded in a 96-well flat bottom microtiter plate at a density of 5×10^4 cells/well in 100 μL of culture medium in triplicates and were incubated for 18 hours before treated with tested compounds. Cells were treated with 10 μM of SCM-198, **11f**, **14f**, **14o** and 1μM of **14o**, respectively for 4 hours before stimulation with H_2O_2 for another 1 hour. Control cells were treated with same volume of DMSO and model cells were treated with H_2O_2 without pre-incubation of compounds. After treatments, collect the medium, the left was washed with PBS for 3 times. Cells were lysed with cell lysis buffer and the protein concentration was determined with BCA colorimetric method. For each sample, add 50 μL of culture supernatant into 50 μL reconstituted 2X LDH assay buffer. Protected the assay plate from light and incubated the plate at room temperature (22-25 °C) for 10-30 min. Absorbance between 490-520 nm was measured. The reading from the control and test wells is subtracted with the reading from the medium alone control wells. The relative LDH activity was calculated according to the following formula:

$$\text{Activity\%} = \frac{(\text{Test well OD} - \text{Medium alone well OD})}{\text{Test well protein content}} \Big/ \frac{(\text{Model well OD} - \text{Medium alone well OD})}{\text{Model well protein content}}$$

4.5 Determination of MnSOD Activity.

Cells were treated with 10 μM of SCM-198, **11f**, **14f**, **14o** and 1 μM of **14o**, respectively for 4 hours before stimulation with H_2O_2 for another 1 hour. After treatment, cells were lysed and centrifugated at 15,000g for 15 min, the supernatant was removed and total protein concentration was measured using a BCA protein assay kit. The MnSOD activity was measured by inhibiting extracellular and cytosolic Cu/Zn SOD activity with KCN (1 mmol/L) using a CuZn/MnSOD assay kit (WST-8)

(Beyotime, Shanghai, China). Briefly, WST-8, a highly water-soluble tetrazolium salt, can be oxidized to formazan dye by cellular superoxide anion, and the reaction could be inhibited by SOD. The activity of SOD was thus determined by colorimetric analysis of the formazan dye. One unit of SOD activity was defined as the amount causing 50% inhibition of the initial rate of reduction of WST-8. MnSOD activity was calculated in terms of protein content (U/mg).

4.6 Detection of Mitochondrial Membrane Potential (Δψm) by JC-1 Staining.

Δψm was determined with the dual-emission mitochondrial dye JC-1. H9c2 cells were pre-treated with 1 μM **14o** or 10 μM SCM-198 for 4 h prior to H_2O_2 treatment (400 nM). After incubation, medium was removed and cells were washing with cold PBS (pH 7.4) for three times, before incubation with 0.5 μg/mL JC-1 dye for 40 min at 37 °C. The dye was then removed and cells were washed with PBS buffer for three times. Samples were immediately observed under fluorescence microscope. The fluorescent signal of monomers is measured with an excitation wavelength of 490 nm and an emission wavelength of 535 nm. The fluorescent signal of aggregates is detected with an excitation wavelength of 525 nm and an emission wavelength of 600 nm.

4.7 Animal Experiments.

C57BL/6J mice at an age of 8 weeks were purchased from SLAC Laboratory Animal Corporation (Songjiang, Shanghai, China). Mice were housed under conventional conditions, fed standard mouse pellets and water. All animals received human care in accordance with the Guide for the Care and Use of Laboratory Animals, published by the National Institutes of Health (NIH publication no. 85-23, revised 1996). The investigation was approved by Institutional Animal Care and Use Committee of Fudan University. Mice were anesthetized with 2% isoflurane and kept anesthesia with 1% isoflurane. Adequacy of anesthesia was monitored by pedal response. The mice were then cannulated the trachea with a polyethylene tube connected to a respirator with a tidal volume of 0.2 mL (110 breaths/min) and mechanically

ventilated with oxygen-enriched room air mixed with isoflurane by a rodent respirator ventilated (Ugo, Comerio, Italy). A thoracotomy was performed at the fourth intercostal space, hearts were ‘‘popped out’’ from chest and the left anterior descending artery (LAD) was permanently ligated with an 8-0 polypropylene suture under sterile conditions. Sham operated mice underwent the same procedure except that the LAD was left untied. During the surgery, body temperature was maintained constant at 37 °C by a heating pad. Mice were randomly assigned into four groups: Sham operated, **14o** (5 $mg \cdot kg^{-1} \cdot day^{-1}$) with AMI, SCM-198 (10 $mg \cdot kg^{-1} \cdot day^{-1}$) with AMI and AMI groups, with 8-10 mice in each group. We intraperitoneally injected mice with **14o**, SCM-198 or vehicle (saline) for 7 d consecutive days before conduction of acute myocardial infarction injury. After the operation, mice were administrated with SCM-198 or **14o** for another three days until they were sacrificed.

4.8 TCC Staining.

TTC (2,3,5-Triphenyltetrazolium chloride) staining was used to evaluate infarct size. Animals were anaesthetized with isoflurane, exsanguinated by perfusion with normal saline supplemented with 40 mM KCl, and hearts were rapidly removed. Freshly isolated heart were transversely cut into 4-5 slices. The slices were incubated with 1% TTC solution, pH 7.4 at 37 °C for 20 min. Then TTC staining buffer was removed and tissues are fixed in 10% PBS-buffered formalin overnight at 2-8 °C and was photographed. Infarct area was determined by computerized planimetry using ImagePro Plus software (version 6.0, Media Cybernetics, Bethesda, MD, USA). The infarct area was expressed as a percentage of the left ventricular area.

4.9 H&E staining.

The cardiac paraffin sections were dried in oven at 55 ^{o}C for 1-2 hours, deparaffinized with xylene and hydrated by gradient ethanol. After washed with tap water for 5 min, the sections were stained with hematoxylin for 10 min and washed with tap water. To remove the unspecific staining in cytoplasm, the sections were dipped in 0.1% HCl for 5 second and washed with tap water for 3-4 times to remove HCl. After that,

sections were stained with Eosin for 3-5 min and washed with ddH_2O to remove Eosin solution. Then the sections were dehydrated in gradient ethanol and xylene. Finally, the sections were mounted with resinene and covered with a cover glass. Optical microscope was used to observe the structure of cardiac fibrils. The normal myoplasm was stained into deep red and collagen was pink. Cellular nucleus was counter stained into deep blue or purple. Cardiomyocytes subjected with ischemic injury were stained into pale pink and infiltrated with massive fragmented nucleus.

4.10 TUNEL Staining.

TUNEL staining relies on the ability of the enzyme terminal deoxynucleotidyl transferase to incorporate labeled dUTP into free 3'-hydroxyl termini generated by the fragmentation of genomic DNA, which occurs during cells programmed death. In this work, apoptosis was determined with a TUNEL staining kit (Roche Applied Science, Indianapolis, IN) according to the instruction. Besides deparaffinized and hydration, permeabilization of the sections with protease K was necessary for a better staining result. Following proteinase K treatment, slides were washed 3 times with ddH_2O. Endogenous peroxidases was then inactivated by covering sections with 2% hydrogen peroxide for 5 min at room temperature. Slides were washed 3 times with ddH_2O and covered with TdT equilibration buffer for 10 min at room temperature, followed by incubation with TdT reaction buffer for 30 min at 37 ^{o}C. The reaction was stopped, sections were washed 3 times with PBS and nuclear were counter stained with DAPI for 5 min at room temperature. Sections were observed under fluorescence microscope with excitation wavelength at 585-600 nm. TUNEL positive nuclear were in red fluorescence.

4.11 Western Blotting Analysis.

Cells were lysed with lysis buffer containing protease and phosphatase inhibitors cocktail (R&D Systems, Inc., MN, USA) on ice for 20 min, lysates were centrifuged at 13,000 g at 4 °C for 15 min. The protein concentration in the supernatant was determined using the BCA protein assay reagent. Equal amounts of protein (20 μg)

were resolved using sodium dodecyl sulfate-polyacrylamide gel electrophoresis (SDS-PAGE) (8-12% acrylamide gel) and transferred to PVDF Hybond-P membrane. Membranes were blocked with defatted milk for 1 h at room temperature. Membranes were then incubated with primary antibodies against caspase-3, pro-caspase-3, Bcl-2, and GAPDH (CST Inc., MA, USA), with gentle rotation overnight at 4 °C. The primary antibody was removed and the membrane was washed with TBST for 3 times, followed by incubated with secondary antibody for 2 hours at room temperature and chemiluminescent detection.

4.12 Pharmacokinetic Study.

Sprague-Dawley rats were used for the pharmacokinetic study. All animals were kept in an environmentally controlled room at 22 ± 2 °C, relative humidity of 50 ± 10% and approximately 12/12 h light/dark cycle. All mice were randomly assigned to two groups (3 mice per group) for oral administration of 10 mg/kg and intravenous injection of 1 mg/kg **14o**, respectively. Blood samples (0.3 mL) were collected *via* retro-orbital bleeding using heparin as an anticoagulant at 0, 0.5, 1, 1.5, 2, 3, 4, 6, 8, 12, 18, and 24 h after administration of **14o**. Each blood sample was separated by centrifugation at 3,500 rpm for 10 min to harvest the plasma. The obtained plasma samples were transferred to tubes for LC-MS/MS analysis.

4.13 Statistics.

Statistical analyses were performed using Graphpad Prism 8.0 (San Diego, CA, USA). The results were expressed as means ± standard deviations (SD). Unpaired *t*-test was employed to determine the statistical differences between two groups with equal variance, otherwise Mann-Whitney U test was used. One-way ANOVA followed by Tukey's test for post hoc comparison was used for comparison among groups, and results were considered statistically significant at the level of $*p < 0.05$.

Acknowledgements

This work was supported by the National Natural Science Foundation of China

(81900224); Significant weak subject in (Shanghai) Pudong New District (NO.PWZbr2017-15) and Leaders Training Program of Pudong Health Bureau of Shanghai (PWRd2017-11).

Appendix A. Supplementary data

Supplementary data related to this article can be found at

Author Contributions

[1]These authors contributed equally to this work. The manuscript was written through contributions of all authors. All authors have given approval to the final version of the manuscript.

Corresponding Author

*E-mail: yzzhu@must.edu.mo (Y. Z. Zhu)

References

1. E.J. Benjamin, P. Muntner, A. Alonso, M.S. Bittencourt, C.W. Callaway, A.P. Carson, A.M. Chamberlain, A.R. Chang, S. Cheng, S.R. Das, F.N. Delling, L. Djousse, M.S.V. Elkind, J.F. Ferguson, M. Fornage, L.C. Jordan, S.S. Khan, B.M. Kissela, K.L. Knutson, T.W. Kwan, D.T. Lackland, T.T. Lewis, J.H. Lichtman, C.T. Longenecker, M.S. Loop, P.L. Lutsey, S.S. Martin, K. Matsushita, A.E. Moran, M.E. Mussolino, M. O'Flaherty, A. Pandey, A.M. Perak, W.D. Rosamond, G.A. Roth, U.K.A. Sampson, G.M. Satou, E.B. Schroeder, S.H. Shah, N.L. Spartano, A. Stokes, D.L. Tirschwell, C.W. Tsao, M.P. Turakhia, L.B. VanWagner, J.T. Wilkins, S.S. Wong, S.S. Virani, American Heart Association Council on Epidemiology and Prevention Statistics Committee and Stroke Statistics Subcommittee. Heart disease and stroke statistics-2019 update: A report from the American Heart Association, Circulation 139 (2019) e56–e528.
2. Y. Sandoval, A.S Jaffe, Type 2 myocardial infarction JACC review topic of the week, J. Am. Coll. Caediol. 73 (2019) 1846-1860.

3. I. Raber, C.P. McCarthy, M. Vaduganathan, D.L. Bhatt, D.A. Wood, J.G. Cleland, R.S. Blumenthal, J.W. McEvoy, The rise and fall of aspirin in the primary prevention of cardiovascular disease, The Lancet 393 (2019) 2155-2167.
4. A.L. Harvey, R.A. Edrada-Ebel, R.J. Quinn, The re-emergence of natural products for drug discovery in the genomics era, Nat. Rev. Drug. Discov. 14 (2015) 111-129.
5. H. Yao, J. K. Liu, S.T. Xu, Z.Y. Zhu, J.Y. Xu, The structural modification of natural products for novel drug discovery, Expert Opin. Drug Discov. 12 (2017) 121-140.
6. L.L. Miao, Q.M. Zhou, C. Peng, Z.H. Liu, L. Xiong, Leonurus japonicus (Chinese motherwort), an excellent traditional medicine for obstetrical and gynecological diseases: A comprehensive overview, Biomed. Pharmacother. 117 (2019) 109060.
7. Y.Y. Li, Y.K. Lin, X.H. Liu, L. Wang, M. Yu, D.J. Li, Y.Z. Zhu, M.R. Du, Leonurine: from gynecologic medicine to pleiotropic agent, Chin. J. Integr. Med. 26 (2020) 152-160.
8. Q.Y. Zhang, Z.J. Wang, D.M. Sun, Y. Wang, P. Xu, W.J. Wu, X.H. Liu, Y.Z Zhu, Novel therapeutic effects of leonurine on ischemic stroke: new mechanisms of BBB integrity, Oxid. Med. Cell Longev. 2017 (2017) 1-17.
9. Q.Y. Zhang, Z.J. Wang, L. Miao, Y. Wang, L.L. Chang, G. Wei, Y.Z. Zhu, Neuroprotective effect of SCM-198 through stabilizing endothelial cell function, Oxid. Med. Cell Longev. 2019 (2019) 7850154.
10. J. Xu, Q. Zhu, W. He, Y.Z. Zhu, SCM-198 protects ischemic brain injury via accelerating the recovery of brain glucose metabolism ameliorating the damage of neurons and inhibiting the activation of microglia, Int. J. Clin. Exp. Med. 10 (2017) 12925-12933.
11. X.H. Liu, L.L. Pan, Q.H. Gong, Y.Z. Zhu, Antiapoptotic effect of novel compound from Herba leonuri-leonurine (SCM-198): a mechanism through inhibition of mitochondria dysfunction in H9c2 cells, Curr. Pharm. Biotechno. 11 (2010) 895-905.
12. S.S. Luo, X.F. Gu, F.F. Ma, C.H. Liu, Y.Q. Shen, R.W. Ge, Y.Z. Zhu, ZYZ451

protects cardiomyocytes from hypoxia-induced apoptosis via enhancing MnSOD and STAT3 interaction, Free. Radical Bio. Med. 92 (2016) 1-14.

13. D. Yang, W.W. Jia, Y.Z. Zhu, Leonurine, a potential agent of traditional Chinese medicine: recent updates and future perspectives, Nat. Prod. Commun. 11 (2016) 1757-1761.
14. Y.Z. Zhu, W.J. Wu, Q. Zhu, X.H. Liu, Discovery of Leonuri and therapeutical applications: from bench to bedside, Pharmacol. Therapeut. 188 (2018) 26-35.
15. C.H. Liu, X.R. Shi, M.A. Kaium, X.F. Gu, Y.Z. Zhu, Leonurine-cysteine analog conjugates as a new class of multifunctional anti-myocardial ischemia agent, Eur. J. Med. Chem. 46 (2011) 3996-4009.
16. H. Gao, X.H. Yang, X.F. Gu, Y.Z. Zhu, Synthesis and biological evaluation of the codrug of leonurine and aspirin as cardioprotective agents, Bioorg. Med. Chem. Lett. 26 (2016) 4650-4654.
17. Y. Wang, Yang. Cao, Q. Zhu, X.F. Gu, Y.Z. Zhu, The discovery of a novel inhibitor of apoptotic protease activating factor-1 (Apaf-1) for ischemic heart: synthesis, activity and target identification, Sci. Rep. 6 (2016) 29820.
18. C.H. Liu, X.F. Gu, Y.Z. Zhu, Synthesis and biological evaluation of novel leonurine-SPRC conjugate as cardioprotective agents, Bioorg. Med. Chem. Lett. 20 (2010) 6942-6946.
19. C.H. Liu, W. Guo, S. Maerz, X.F. Gu, Y.Z. Zhu, 3,5-Dimethoxy-4-(3-(2-carbonyl-ethyldisulfanyl)-propionyl)-benzoic acid 4-guanidino-butyl ester: a novel twin drug that prevents primary cardiac myocytes from hypoxia-induced apoptosis, Eur. J. Pharmacol. 700 (2013) 118-126.
20. W. Hou, B. Liu, H.T. Xu, Celastrol: Progresses in structure-modifications, structure-activity relationships, pharmacology and toxicology. Eur. J. Med. Chem. 189 (2020) 112081.
21. J. Kim, J. Kim, H. Kook, W.J. Park, PICOT alleviates myocardial ischemia-reperfusion injury by reducing intracellular levels of reactive oxygen species, Biochem. Bioph. Res. Co. 485 (2017) 807-813.
22. H. Yao, S.S. Luo, J.K. Liu, S.W. Xie, Y.P. Liu, J.Y. Xu, Z.Y. Zhu, S.T. Xu,

Controllable thioester-based hydrogen sulfide slow-releasing donors as cardioprotective agents, Chem. Commun. 55 (2019) 6193-6196.

23. A.K. Jain, D. Singh, K. Dubey, R. Maurya, S. Mittal, A.K. Pandey, Chapter 3-Models and methods for in vitro toxicity. In Vitro Toxicology; A. Dhawan, S. Kwon, Eds.; Academic Press: Cambridge, MA, USA, 2018; pp 45-65.
24. D. Candas, J.J. Li, MnSOD in oxidative stress-response-potential regulation via mitochondrial protein influx, Antioxid. Redox. Sign. 20 (2014) 1599-1617.
25. S.J.F. Chong, I.C.C. Low, S Pervaiz, Mitochondrial ROS and involvement of Bcl-2 as a mitochondrial ROS regulator, Mitochondrion 19 (2014) 39-48.
26. C.M. Pfeffer, A.T. Singh, Apoptosis: a target for anticancer therapy, Int. J. Mol Sci. 19 (2018) 448.
27. J.M. Li, H. Zhou, Q. Cai, G.X. Xiao, Role of mitochondrial dysfunction in hydrogen peroxide-induced apoptosis of intestinal epithelial cells, World J. Gastroenterolo. 9 (2003) 562-567.
28. R. Suguro, S. Chen, D. Yang, Z. Yang, L. Miao, W. Wu, W. Zeng, X. Liu, Y.Z. Zhu, Anti-hypercholesterolemic effects and a good safety profile of SCM-198 in animals: from ApoE knockout mice to Rhesus monkeys, Front. Pharmacol. 9 (2018) 1468.
29. M. Bonora, M.R. Wieckowski, D.A. Sinclair, G. Kroemer, P. Pinton, L. Galluzzi, Targeting mitochondria for cardiovascular disorders: therapeutic potential and obstacles, Nat. Rev. Cardiol. 16 (2019) 33-55.
30. Y.Q. Wen, L.Y. Gong, L. Wang, N. Zhao, Q. Sun, M.O. Kamara, H.Y. Ma, F.H. Meng, Comparative pharmacokinetics study of leonurine and stachydrine in normal rats and rats with cold-stagnation and blood-stasis primary dysmenorrhea after the administration of Leonurus japonicas houtt electuary, J. Sep. Sci. 42 (2019) 1725-1732.
31. E. Pfeiffer, S.I. Hoehle, S.G. Walch, A. Riess, A.M. Sólyom, M. Metzler, Curcuminoids form reactive glucuronides in vitro, J. Agr. Food Chem. 55 (2007) 538-544.

1. 35 Analogs of SCM-198 were designed, synthesized and biologically evaluated.
2. Analog **14o** significantly reduced cardiomyocytes apoptosis.
3. The mice pretreated with **14o** had much lower infarct size than that of SCM-198.
4. **14o** might be a potential cardioprotective agent to treat acute myocardial infarction.

Declaration of interests

☒ The authors declare that they have no known competing financial interests or personal relationships that could have appeared to influence the work reported in this paper.

☐The authors declare the following financial interests/personal relationships which may be considered as potential competing interests: